

Article citation info:

Balakrishnan K, Mani I, Sankaran D, Predicting the overall equipment efficiency of core drill rigs in mining using ANN and improving it using MCDM, *Eksploracja i Niezawodność – Maintenance and Reliability* 2023: 25(3) <http://doi.org/10.17531/ein/169581>

Predicting the overall equipment efficiency of core drill rigs in mining using ANN and improving it using MCDM

Indexed by:



Kirubakaran Balakrishnan^{a,*}, Ilankumaran Mani^b, Durairaj Sankaran^c

^a AVS College of Technology, Department of Mechanical Engineering, Chinnagoundapuram, Salem, Tamil Nadu, India

^b Department of Mechanical Engineering, Knowledge Institute of Technology, NH544, Kakapalayam, Salem, India

^c Department of Electrical Engineering, Annaporana Engineering College, Salem, India

Highlights

- Combined Box Jenkins and artificial neural network model was used to improve Overall Equipment Efficiency of Core Drill rigs.
- Combined model achieved better prediction of overall equipment effectiveness, compared to auto regressive moving average and non linear auto regressive neural network model.
- Response surface methodology was found to be effective in optimizing and improving the overall equipment efficiency.

Abstract

In this manuscript, an attempt has been made to predict and improve the overall equipment effectiveness of core drill rigs. A combined Box–Jenkins and artificial neural network model was used to develop a three parameter model (drill pushing pressure, drill penetration rate & average pillar drill pit cycle time) for predicting effectiveness. The overall equipment efficiency of core drill rigs. The values of mean average percentage error, root mean square error, normalized root mean square error, men bias error, normalized mean biased error and coefficient of determination values were found to be 9.462%, 17.378%, 0.194, 0.96%, 0.0014 and 0.923. Empirical relationships were developed between the input and output parameters and its effectiveness were evaluated using analysis of variance. For attaining 74.9% effectiveness, the optimized values of pushing pressure, penetration rate and average pillar drill pit cycle time were predicted to be 101.7 bar, 0.94 m/min and 272 min, which was validated. Interactions, perturbations and sensitivity analysis were conducted.

Keywords

artificial neural network, response surface methodology, core drill, overall equipment efficiency, Box-Jenkins

This is an open access article under the CC BY license (<https://creativecommons.org/licenses/by/4.0/>)

1. Introduction

In mining sectors, selection of equipments is important for ensuring hassle free production [80]. Important operations in mining involve drilling, loading and hauling. Core drill rigs are being used in tough terrain and mining locations. Drilling operations should be optimized for improving the utilization of the drill rigs [75]. It is important to identify the priority factors pertaining to drill rigs. Effective usage of equipment depends on its availability and age [78]. Identification of the important equipment factors pertaining to drill rigs help in reducing the

maintenance and repair costs [101]. Steps should be taken for improving the economic feasibility of using core drills in unknown and tough terrains [69]. The importance of mining has increased in recent years due to enormous demand for metal ores. Attempts to improve the overall equipment effectiveness are welcomed as they help to improve production without standby and repairs [66]. The life cycle of mining equipments can be improved by ensuring proper maintenance of important parts and components [79]. In addition to increased working

(*) Corresponding author.

E-mail addresses:

K. Balakrishnan (ORCID: 0000-0002-9218-0664) kirubabalu@gmail.com, I. Mani (ORCID: 0000-0001-7378-6313) mikmech@kiot.ac.in, D. Sankaran (ORCID: 0000-0001-6455-3913) durairajeebe@gmail.com

time and profits, better maintained equipments ensure reduced accidents. Improvement in equipment reliability helps in improving safety to the manpower and other nearby components [51]. As mining are always done in remote and tough terrains, it is important to prevent undesirable accidents during drilling operations. Overall improvement in equipment maintenance helps to reduce repair time and equipment downtime [44].

Even though sophisticated core drilling equipments are being manufactured, the complexity of core drilling makes the operation tough. Core drilling operation involves more of grinding and hence time duration would be more [25]. This increased duration of contact between the tool and the surface induces tool damage [33], bending of segment holders [109], excessive drill vibration [91], slurry wear and barrel cracking [7]. The vital site parameters and sensitive equipment details are to be known so that the equipment can be run in an efficient manner [5]. For research in mining, knowledge about the parameters involved in the equipment functioning are important [27]. In core drilling equipment, proper control over its operating process parameters should be exercised for improved equipment performance. Pushing pressure of the core drillers [90], penetration rate in the mining region [93] and rotational pressure of the core drill drum determines the duration and shape of the pillar drill face and stope holes. Time duration,, size, repeatability, precision of the drill holes and the overall drill efficiency depends on the important core drill process parameters [110]. By predicting Overall Equipment Effectiveness (OEE) of the equipment, estimation of product quantities, man power, duration and other important aspects involved in mining can be done [20]. Unfortunately, there are limited resources available for evaluating OEE, which induces fluctuations in project estimation and projections [8]. Approaches for predicting and improving OEE are important to increase the accuracy of the operations [54]. Lot of experiments was conducted in the past, for improving the efficiency of core drilling. Effect of the bit drill modification on rock breaking efficiency was studied [95]. In core drilling, incorporation of pulse flushing mode improved the drilling efficiency [13]. The effect of core drill design modifications on ice core drill efficiency was observed [92]. A modified pressure holding technology was used to improve core drilling in coal mines [22].

Design modifications, attachments and process alterations have been done to improve the existing functioning of core drillers. The efficiency of core drillers was studied on conducting orthogonal experiments [95]. Intermittent characteristics of mining operations make its workability limited and hence, predicting the efficiencies of the equipments is well sought for [76]. Researchers have used different artificial neural network (ANN) models and Box Jenkins for predicting the output of systems. Box Jenkins Linear Auto-Regressive Moving Average (LARMA) models are successfully used for prediction of complex systems as they are very flexible [12].

Researchers found a lot of similarities between ANN and Box Jenkins model. Non stationery time series is the criteria differentiating ANN and Box Jenkins [98]. For adjusting and predicting stationary time series, autoregressive integrated moving average was found to be better, compared to other traditional models [62]. For increasing the accuracy of the prediction models, regression model was combined with Auto Regressive Moving Average (ARMA) technique [37]. ARMA model was not accurate in predicting non-linear models. On combining ANN techniques with ARMA model, even with non-linear data, the prediction was very high. ANN models are highly recommended for predicting system efficiencies [14]. ANN models use different non-linear and independent variable factors to accurately predict the desired responses. Researchers found fuzzy logics incorporated ANN models to be effective in predicting OEE and performance assessment [24]. Stability of rock surrounded tunnels was identified by combining auto-regressive algorithm with firefly algorithm [74]. Prediction accuracy indicators such as mean bias error, determination coefficient and relative root mean square error were used for identifying the accuracy of developed artificial neural network models [86]. In mining, adaptive neuro-fuzzy interference systems were incorporated with multiple regression algorithms for improving the drilling efficiency of core drillers using diamond bits [6]. Support vector machine algorithm was used to identify geographical locations rich in mineral ores [1]. The important technological process parameters involved in core drilling of mining rocks were identified by using fuzzy based least square support vector machine algorithm [111]. On comparing the prediction accuracy of models developed by using support vector machine algorithm with other artificial

neural network algorithms, the coefficient of determination and root mean square error values indicated that fuzzy based least square support vector machine algorithm was better [16]. Genetic algorithm improved using fuzzy logic helped in improving the control on back pressure on wellheads [53]. Statistical indicators were found to be efficient for comparing the efficiencies of Adaptive Neuro-Fuzzy Inference System (ANFIS) and ANN models [85]. It was observed that the prediction accuracy of single forecasting models were relatively lower than the prediction accuracy of combined models [56]. Time delay neural networks (TDNN) were found to be effective for monitoring wear of drilling tools. Non linear evaluation of systems was efficient on using TDNN [88]. Dynamic forecasting was found to be effective on combining neuro-fuzzy model with Kalman filter model and ARMA model [11]. For extraction and clustering of data from time-series, k-means method was effective. Non linear auto-regressive neural networks were combined with k-means clustering for improving the prediction accuracy [77]. Research on developing complex predictions in isolated regions indicated that machine learning algorithms with artificial intelligence had very accurate predictions [41].

Optimization techniques help in achieving the desired goal with minimum number of experiments. Response surface methodology (RSM) technique was effective in removing uranium rich mine water [70]. RSM was used for reducing erosion wear of ocean mining pump [40]. For optimizing the explosion and drill pattern in rock tunneling, RSM was used [2]. Three variables such as profit, physical and economic life determines the overall equipment life. Physical and economic life calculations are important for identifying the replacement time of that equipment [82]. For evaluating the profit life of equipment, the important factors taken into consideration are repairs, time-offs, devaluation and maintenance costs [84]. The cost of procurement of new equipment should be justified before replacement. The profit earned by the equipment before its replacement should cover its associated productivity, repair and maintenance costs during its effective operational period [102]. Thus, in mining, knowledge and operation sequences help in predicting the overall effective working time of equipment [108]. This helps in arranging repairs or replacement of the equipment. During continuous working of equipments in

mining areas, apart from recorded data, a lot of considerations should be taken care of, for hassle free working. Identification and prediction of equipment efficiency is useful in remote mining operations. Even though lot of studies has been conducted in mining equipments, overall equipment effectiveness is a very important aspect for ensuring safety and productivity. On conducting an exhaustive literature survey, it was observed that literatures on estimation and improving overall equipment effectiveness of mining equipments were nil. Hence, in this investigation, an attempt has been made to develop Box Jenkins combined ANN model for predicting the Overall Equipment Effectiveness (OEE) of core drill rigs. Using RSM the drilling parameters were optimized for improving OEE of the core drill rigs.

2. MATERIALS & METHODS

2.1 Mining equipment and parameters for evaluating Overall Equipment Effectiveness of drill rigs

The mining equipment considered in this research was core drill rigs used in Vermiculite and Quartz mines near Salem, Dharmapuri, Namakkal and Tiruchirappalli districts of Tamil Nadu, India. The core drill rigs were associated with M/s. Tamil Nadu Magnesite Ltd., Salem, Tamil Nadu, India. The drill rigs were heavy type, with toughened steel drill bits. The drilling equipment is shown in Figure 1.



Figure. 1. Core drill rig equipment used in mining.

For evaluating OEE, physical, economic and profit life of the core drill rigs were used. The service life of drill rigs were taken as its physical life. All forms of repairs and maintenance affect the physical life of the equipment. Preventive maintenance, routine servicing and proper working conditions help to increase the physical life of equipment [81]. Profit life is the duration till which the equipment earns more than its

repair and maintenance expenditures. It helps the owners to determine when to repair and when to replace the equipment. It is the period in which profits are booked while operating the equipment. After this period, it is advisable to replace the equipment, as it is no longer profitable. This helps mining companies to predict and improve production efficiency [68]. Economic life of equipment is the working duration when the purchase and maintenance costs are equal to the cost of operation. Expiry of economic life is an indication to replace the equipment [48]. For evaluating life cycle of the drill rigs, operational costs were considered. For core drill rigs, the operational costs included labor charges of drill operators, maintenance costs, fuel, tire, drill bit breakage replacement and repair costs [99]. For determining OEE of the core drill rigs, a modified Nakajima equation developed by Samatamba et al 2019 [65], has been used. The equation developed by Samatamba et al 2019, is shown below

$$OEE = A \times UR \times PE \quad (1)$$

In the above equation, A is availability, UR is the Utilization Rate of the equipment and PE is the Production Efficiency of the equipment. The equations for availability (A), Utilization Rate (UR) and Production Efficiency (PE) are shown as follows

$$A = \frac{PAT - T_D}{TAT} \times 100 \quad (2)$$

In Eq. 2., PAD is the planned available time, T_D is the total downtime and TAT is the total available time.

$$UR = \frac{T_o - I_H - T_D}{T_o - T_D} \times 100 \quad (3)$$

In Eq. 3., T_o is the total output, I_H is the idle time in hrs.

PE was evaluated after taking the hole deviations and ruptures into consideration.

$$PE = \frac{APT}{(ART - I_H) \times R_c} \times 100 \quad (4)$$

In Eq. 4, APT is the actual production time, I_H is the idle hours and R_c is the rated capacity.

For evaluating equipment availability, three shifts of 8 hrs per day were considered. The actual data record (record sheet) from the drill operators were taken for evaluation. Equipment utilization was recorded from the equipment gate pass in and out registers. During a shift, 7 rigs were used and one equipment was placed in standby. The time lag between starting of equipment, replacing and repair were recorded to evaluate the

mean time between shutdowns and failures. For the collected data, production efficiency was calculated. The primary data (questionnaires to operators, mining and maintenance engineers) and secondary data (checklists, trip sheets) were collected and used in this investigation. Drilling operation starts when the pillar drill tip touches the top surface of the mining area. After evaluating the data collected, Overall Maintenance Index (OMI) was calculated between 0 and 1. It comprised of planned maintenance shutdown, damage assessment, maintenance time, breakdown maintenance, oil maintenance, tire maintenance and frame body maintenance. Other variables considered for this investigation for the drill rigs were Pushing Pressure (PP) in bar, Rotational Pressure (RP) in bar, Penetration Rate (PR) in m/min, Idle Time (IT) in hrs, Operated Time (OT) in hrs, Utilization Rate (UT), Average Pillar Drill Pit Cycle Time (APDPCT) in mins, Average Time to Pillar Drill One Face Hole (ATPDFH), Average Time for Drilling One Stope Hole (ATDSH) in mins, Mean Time Before Failure (MTBF) in hrs, Productive Time (PT) in hrs, Availability (A) in %, Utilization Rate in %, Production Efficiency in % and Overall Equipment Effectiveness (OEE) in %. During drilling the pit, support fixtures were extended to prevent equipment vibration. After drilling, the pillar drilling bit was retracted. Before moving the equipment to another place, the support fixtures were also retracted. The Average Pillar Drill Pit Cycle Time (APDPCT) [97] was calculated according to the following equation

$$APDPCT = ADT_1 + AST + D \quad (5)$$

In Eq. 5, ADT₁ is the average time taken for drilling one hole, ACT is the Average Settling Time and D is delay

The Average Time to Pillar drill one Face Hole (ATPDFH) was calculated according to Eq. 6 and the Average time taken for drilling on Stope hole (ATDSH) was calculated according to Eq. 7.

$$ATPDFH = ADT_1 + ST + D \quad (6)$$

$$ATDSH = \frac{\sum_1^n TTDH + ST + D}{n} \quad (7)$$

In the above equations, ST is settling time, TTDH is the total time taken for drilling holes and n is the number of holes.

2.2 Box-Jenkins Auto Regressive Moving Average model for predicting OEE

For predicting OEE of core drill rigs, Auto Regressive Moving

Average (ARMA) model was developed with Box-Jenkins technique. Hybridization has been successful in improving the prediction accuracies. Accurate predictions with non-linear and non-compensatory relationships [96] could be obtained by using hybridization. Hybridization of ANN with other models helps in improving the performance of the neural networks [83]. Increase in flexibility was observed on using hybrid models in ANN [94]. ARMA model consists of two components. The first one is the auto-regressive component and the second one is the moving average component. In combined form, they are represented as ARMA (a, b), where a & b are order of autoregressive component and moving average component respectively. The general equation of ARMA model is given below

$$R_t = \sum_{i=1}^p \phi_i R_{t-1} - \sum_{j=1}^q \theta_j e_{t-j} + e_t \quad (8)$$

In Eq. 8, autoregressive parameters are indicated as ϕ_i and the moving average parameters are indicated as θ_j . Noise of the

equation is denoted as e_t . ARMA model was developed in three stages. In the first stage, identification of the best fit on time series was done according to Auto-Correlation Function (ACRF) and Partial Auto-Correlation Function (PACRF) [28]. Auto-Correlation function is used for identifying the relationship between the present set and preceding set of data points. It also helps in measuring self similarity [104]. Partial Auto-Correlation function helps in identifying the partial correlation between the present and past observations under its own regressive lags [61]. Depending on the pattern variations in ACRF values, time series values are considered to be stationary or non stationary [64]. If sudden decrease and flattening of ACRF values was observed, the time series were considered to be stationery. On the other hand, if ACRF values do not flatten quickly, then the time series were considered to be non-stationary. Depending on the behavior of ACRF and PACRF values, the choice of ARMA model is indicated in Table 1.

Table 1. Decision factors for ARMA model based on the behavior of PACRF and ACRF values.

Model	ACRF	PACRF
AR (a)	When projection diminishes toward zero and oscillations in coefficients occur	When projection diminishes after lag a
MA(b)	When projection diminishes to zero after lag q	When projection diminishes towards zero and oscillations in coefficients occur
ARMA(a,b)	When projection diminishes to zero after lag b	When projection diminishes to zero after lag a

The first stage is completed after identification of the model. In the second stage, estimation of the parameters is done. The third stage of Box Jenkins method is verification. There are different testing methods available for verification. Breusch–Godfrey test is used for validity assessment of modeling assumptions [4]. Durbin Watson test is used for evaluating autocorrelation in residuals of a statistical model. From 0 to 4, Durban-Watson statistic is used for detecting autocorrelation between the samples [59]. Ljung-Box test is used for determining whether the autocorrelations of a time series varies from zero. Durbin Watson can be used only for identifying auto regression of the first order and lag of 1. For lag value greater than 1, Ljung Box test can be effectively used. Ljung-box technique uses null hypothesis for checking if there are no residual autocorrelations. Hence, in this investigation, Ljung-Box test was used [38]. The Ljung-box equation for identifying nil residual auto-correlations is shown below

$$L = n(n + 2) \sum_{k=1}^h \frac{\rho_k^2}{n-k} \quad (9)$$

In Eq. 9, auto-correlation coefficient at lag k is denoted as ρ_k . With degree of freedom f of χ^2 distribution, rejection of hypothesis is done when the value of Q is greater than 95% of χ^2 distribution. The sequence of operations in Box Jenkins is shown in Figure 2 (a).

2.3 Artificial Neural Network model for predicting OEE

For prediction model development, advanced neural networks such as Artificial Neural Networks and Polynomial Neural Networks are used. Artificial Neural Network (ANN) is an advanced methodology used for predicting the responses of complex and non-linear systems. ANN models use intelligent human like decision making strategies for evaluation of input data without biased assumptions and imposing [30]. Polynomial Neural Networks is a self organizing network, which can be used for developing prediction models [17]. It consists of dynamic layers. Growth of layers and its structure depends on the learning process. On using polynomial models, a reduction in interpolation and extrapolation aspects were observed [55].

For predicting OEE, a lot of dynamic parameters are involved. The relationship between the processes parameters are complex. For analyzing such complex models, ANN was found to be accurate. Hence, in this investigation, ANN was used for developing the prediction model. Neural networks have input layers for receiving data and output layers for delivering the processed data. Hidden layers are used for linking input with output layers [47]. Hidden layers help in improving the performance of a model. Even for highly complex models, hidden layers improve the predictability and accuracy to a great extent [105]. The consecutive layers are connected to each other by using neurons. Schematic representation of ANN model for estimating OEE of the core drill rigs is shown in Figure 2 (b).

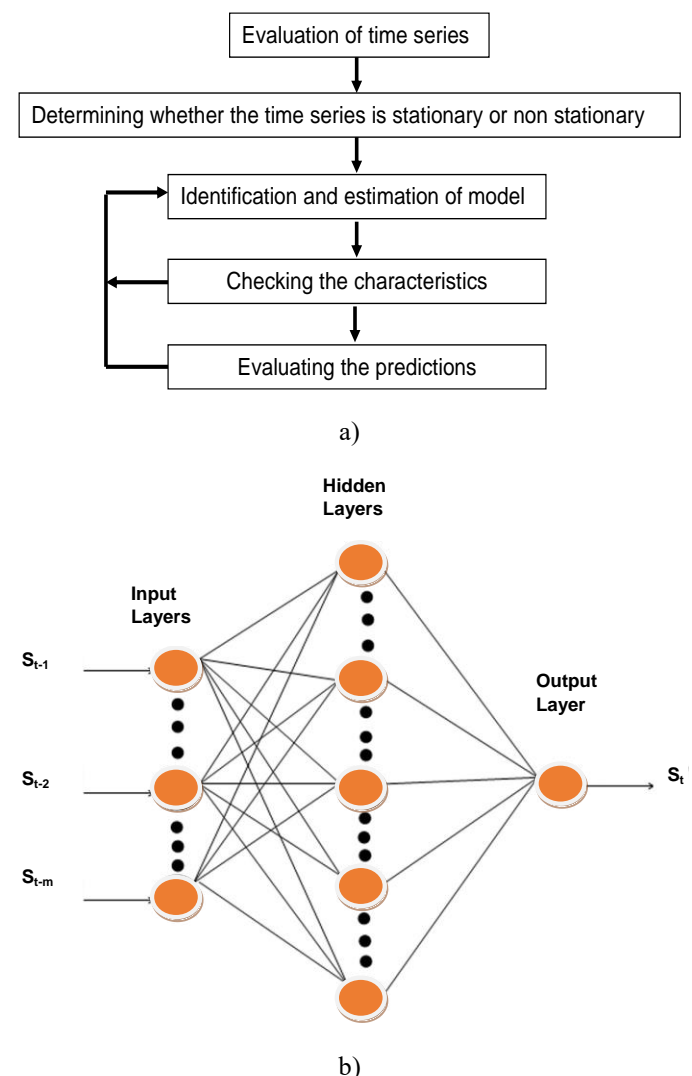


Figure 2. (a) Sequence of operations in Box-Jenkins algorithm, (b) ANN model for estimating OEE.

There are different algorithms which can be used for learning process. Deep belief network consists of multiple layered variables. Using this network reconstruction of inputs

can be done without supervision. Compared to Multi Layer Perceptron, deep belief network is more expensive, requires classifiers and a large volume of data for accurate performance [19]. Restricted Boltzmann Machine algorithms are used for generation of artificial neural network model using a set of inputs, with probability distribution. Compared to Multi Layer Perceptron, Restricted Boltzmann Machine algorithms exhibit more difficulty in weight adjustment and estimating gradient functions [19]. Convolution Neural Network models are used for visualization models and analyzing image based data [52]. Compared to Multi Layer Perceptron, convolution neural network are slow in executing calculations, need a large quantity of data for increasing accuracy and exhibit low component understanding capability [107]. Recurrent Neural Network model uses the output from the previous step as input to improve the prediction accuracy. A lot of memory is required for remembering the previous values of output. Training of recurrent neural network is a very tough task and it cannot process long sequences [50]. Hence, in this investigation, Multi Layer Perceptron (MLP) network based learning with feed forward back propagation algorithm was used. MLP network learning was selected as it found to be better for estimating responses of dynamic systems with appreciably high accuracies [10]. Non-linear auto regressive network (NLARNN) based model with feedback was used in this study. It is a recurrent network based linear autoregressive model, which includes several network layers. NLARNN model involves past values of the time series for estimating the next consecutive values. The values were determined according to the following equation

$$S_t = f(S_{t-1} + S_{t-2} + \dots + S_{t-d}) \quad (10)$$

There are different algorithms available for adjustment of model weights and training. Gradient algorithm is an optimization method for identifying the local minima. Gradient descent can be used only if the entire function is fully differentiable [106]. In other cases, gradient cannot be defined. Newton method is used for addressing non-linear problems. In Newton method, for achieving convergence, the iterations should begin very close to the searched for zero values. Conjugate gradient method is used to provide solutions for linear systems [32]. Conjugate gradient method needs a lot of cycles for reaching minimization, which limits its

implementation [43]. Quasi-Newton method is an alternative to Newton method for identifying local zeros, maxima and minima. It is mandatory that the Hessian matrix should be positive and the function should be differentiable twice. Only then, Quasi-Newton method can be applied [39]. At higher dimensions and for solving minimization bases problems, Levenberg Marquardt (LM) algorithm is generally used. This LM algorithm involves both the concepts of Newton and gradient algorithm. For training and adjustment of weights, LM algorithm was found to be better than other algorithms [57]. Hence, in this investigation, for NLARNN model, LM algorithm was used.

2.3 Combined Box-Jenkins with ANN model

For improving the prediction and estimation accuracy, a combination of linear and non-linear systems was done. In this investigation, for capturing linear information, Auto Regressive Moving Average model was used and for capturing non-linear information, ANN model was used. A combined model was developed by Gairaa et al. 2016 [31], and the expressions are given below

$$Y_t = LC_t + NLC_t \quad (11)$$

In Eq. 11, the original time series is shown as y_t . In Eq. 11, the linear component is denoted as LC_t and the non linear component is denoted as NLC_t . In the first stage, ARMA was performed for modeling the linear aspects of the core drill rig process variables. The non-linear aspects were accumulated in the residuals. From linear fit, the residuals r_t was evaluated from the following equation

$$r_t = y_t - |EV|_t \quad (12)$$

In the above equation, the estimation value of ARMA is denoted as EV_t . In the next stage, the residuals of ARMA model were modeled by using NLARNN technique. Equation for representing ARMA models using NLARNN is shown below

$$r_t = f(r_{t-1}, r_{1-2}, \dots, r_{t-d}) + \varepsilon_t \quad (13)$$

In Eq.13, the non linear function is shown as f and random error is shown as ε_t . The equation of combined hybrid (CH_t) model developed for integrating the linear and non-linear components is shown below

$$|CH_t| = |EV_t| + |NLC_t| \quad (14)$$

The sequence of the combined hybrid model is shown in Figure 3.

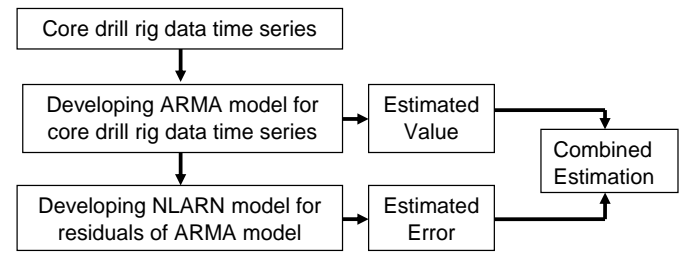


Figure 3. Sequence of operations in combined hybrid model.

2.4 Evaluating the performance of the developed hybrid model

By using statistical indicators, the accuracy of the developed model was ascertained. The performance indicators such as coefficient of determination (R^2), mean bias error (MBE), normalized MBE (n-MBE), root mean square error (RMSE), normalized root mean square error (n-RMSE) and mean average percentage error (MAPE) were used [34]. The equations for evaluating the performance indicators are shown below

$$R^2 = \frac{\sum_{i=1}^D (ev_i - mv_i)^2}{\sum_{i=1}^D (\bar{ev}_i - \bar{mv}_i)^2} \quad (15)$$

$$RMSE = \sqrt{\sum_{i=1}^D \frac{(e_i - m_i)^2}{D}} \quad (16)$$

$$nRMSE = [\sum_{i=1}^D (ev_i - mv_i)^2 / D] / mv \quad (17)$$

$$MBE = \sum_{i=1}^D (ev_i - mv_i)^2 / D \quad (18)$$

$$nMBE = \sum_{i=1}^D (ev_i - mv_i)^2 / D \bar{ev} \quad (19)$$

$$MAPE = \sum_{i=1}^D ((ev_i - mv_i) / D mv_i) \times 100 \quad (20)$$

In the above equations, the estimated values are indicated as ev_i and the measured values are indicated as mv_i . The average of the estimated and the measured values are indicated as \bar{ev} and \bar{mv} respectively.

2.5 Optimizing the important drill rig process parameters for improving OEE

For developing empirical relationship between the input parameters and output responses, different models such as Box Behnken and Central Composite Design models are used. Box Behnken models are used for generating response surfaces of higher orders, during optimization [18]. While using Box Behnken, if there are any missing runs, the dependability of the model reduces drastically. Central composite design is found to be a reliable method for building a quadratic model of second order [89]. There are different techniques which can be used for multi criteria decision making. Genetic algorithm uses natural selection criteria for identifying the best [15]. Hill climbing uses

the concept of moving towards elevation for identifying the optimum solution [3]. Vikor algorithm uses ranking to identify important process variables according to the initially assigned weights [21]. Travelling salesman is a graphical computation method for utilizing all the given routs with minimal distance [35]. Response surface methodology uses statistical and mathematical techniques for identifying the relationship between dependent variables and output responses [100]. For improving OEE to the maximum possible limit, the important core drilling process parameters should be identified for achieving the desired results. The range of the variables is high and minimization of error should be given priority for improving the accuracy of the prediction. Since response surface methodology uses advanced mathematical techniques for identifying the parameters to improve response, it was selected for this investigation. In this investigation RSM was used to optimize the important drill rig process parameters by developing central composite design model. Using experimental trials, the feasible limits of the important drill rig process parameters were identified. Within the feasible limits of process parameters, twenty different combinations were developed by using central composite design model. The twenty combinational runs were developed by using 8 design, 6 star and central points. With each process parameter combinations, core drilling experiments were conducted and from the results obtained, OEE was calculated and recorded. In the twenty process parameter combinations, six repetitive experiments were used for eliminating errors induced during the core drilling experiments. Second order regression equations were used to establish empirical relationships between the input variables and OEE. The closeness between the predicted and actual OEE was identified. For identifying the differences in variances, techniques such as analysis of variance (ANOVA), Kruskal-Wallis and Mann Whitney U tests are being used. Kruskal-Wallis testing is a non-parametric method for determining the origin of the samples and comparing independent samples [46]. Analysis of variance (ANOVA) method is used to determine the differences in mean values of more than two groups [9]. For evaluating samples with multiple scales, independent factors, within a particular range, ANOVA is found to be better than other methods. The significance of the developed core drill rig performance improvement model was evaluated by using

Analysis of Variance (ANOVA). Two way type III ANOVA was used for evaluation.

Mann Whitney U method is a non-parametric testing method for understanding the relationship between values of two populations [49]. For evaluating the closeness between the predicted OEE and the actual OEE values, Mann Whitney U and ANOVA method was used. Mann Whitney U test was conducted in two steps. In the first step, the values are sorted from the smallest to largest. In the second step, summation of the rank scores for each group is done. Using the following equation, the score value is calculated

$$E(U) = \frac{n_u(N+1)}{2} \quad (21)$$

In the above equation, E(U) is the expectation value of U, the total number of examined samples is denoted as n_u , the total samples is denoted as N, where

$$N = n_1 + n_2 \quad (22)$$

A score value of z is calculated using the following equation

$$z = \frac{U_{max}}{\sqrt{\frac{n_1 n_2 (N+1)}{20}}} \quad (23)$$

In the above equation, the value of maximum rank is denoted as U_{max} , the number of independent samples of the two categories is denoted as n_1 and n_2 . Contours and 3-D surface plots were developed by using RSM to optimize the input variable to predict maximum possible OEE. Using validation experiments, the predictability of the developed core drill rig model was validated. Interactions and perturbation plots were developed and sensitivity analysis was conducted to rank the core drill parameters.

3. RESULTS AND DISCUSSIONS

3.1 Estimation and prediction of OEE using Box-Jenkins ANN hybrid model

For core drilling, the data collected for the process variables such as Overall Maintenance Index (OMI), Pushing Pressure (PP) in bar, Rotational Pressure (RP) in bar, Penetration Rate (PR) in m/min, Idle Time (IT) in hrs, Operated Time (OT) in hrs, Average Pillar Drill Pit Cycle Time (APDPCT) in mins, Average Time to Pillar Drill One Face Hole (ATPDFH), Average Time for Drilling One Stope Hole (ATDSH) in mins, Mean Time Before Failure (MTBF) in hrs, Productive Time (PT) in hrs, Availability (A) in %, Utilization Rate (UR) in %,

Production Efficiency (PE) in % and Overall Equipment

Effectiveness (OEE) in % are shown in Figure 4.

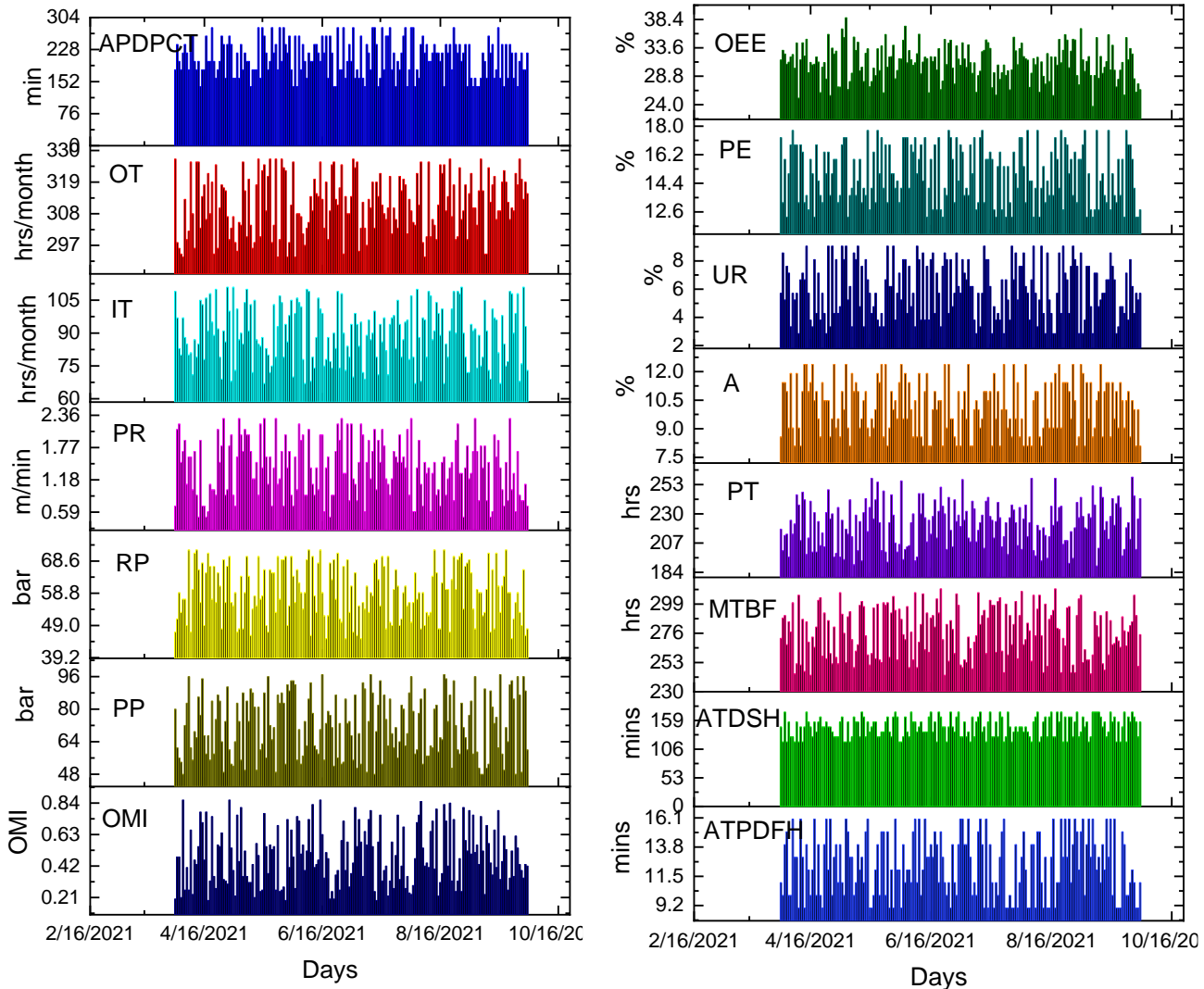


Figure 4. Data collected for the investigation.

As the data obtained regarding OEE of core drill rigs are not stationary, ratio of Absolute Total Effective Equipment Performance ($TEEP_a$) and OEE was taken as the Effectiveness Index (EI) ratio. As $TEEP_a$ identifies the actual production capacity, it was used to convert the time series into a stationary one. The time series should be stationary if ARMA has to be implemented. Auto Regressive Moving average (ARMA) was chosen over Auto Regressive integrated Moving Average (ARIMA) because, in ARIMA differencing should be incorporated for converting non-stationary to stationary time series model. In certain cases, second differencing should be done for conversion to stationary time series. In this investigation, the data collected and evaluated (APDPCT, OT, IT, PR, RP, PP, OMI, OEE, PE, UR, A, PT, MTBF, ATDSH, ATPDF) were collected from defined sources. As conversion of non-stationary time series to stationary series was done by

calculating the effectiveness index, ARMA method was selected in this investigation for quick and accurate prediction with high convergence [60].

The equation for EI has been shown below

$$EI = \frac{TEEP_a}{OEE} \quad (24)$$

In the above equation the Absolute Total Effective Equipment Performance is denoted as $TEEP_a$. The formula for evaluating $TEEP_a$ is shown below

$$TEEP_a = \frac{P \times Q \times APT}{AT} \quad (25)$$

In the above equations, Quality is termed as Q, Actual Production Time is denoted as APT and All Time is denoted as AT. The variations in EI are shown in Figure 5. The corresponding Auto-Correlation Function (ACRF) and Partial Auto Correlation Function (PACRF) were plotted for EI and are

shown in Figure 6 (a) and Figure 6 (b) respectively.

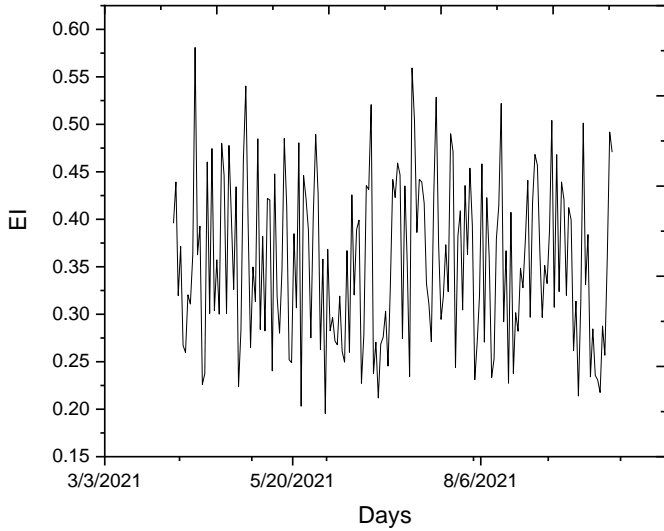
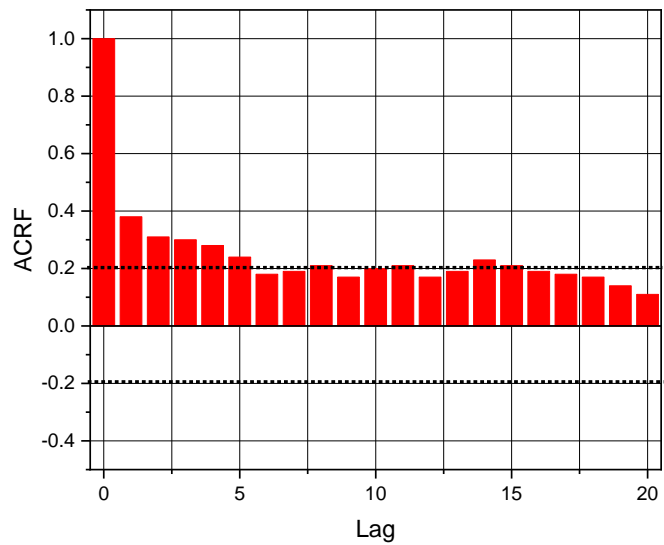
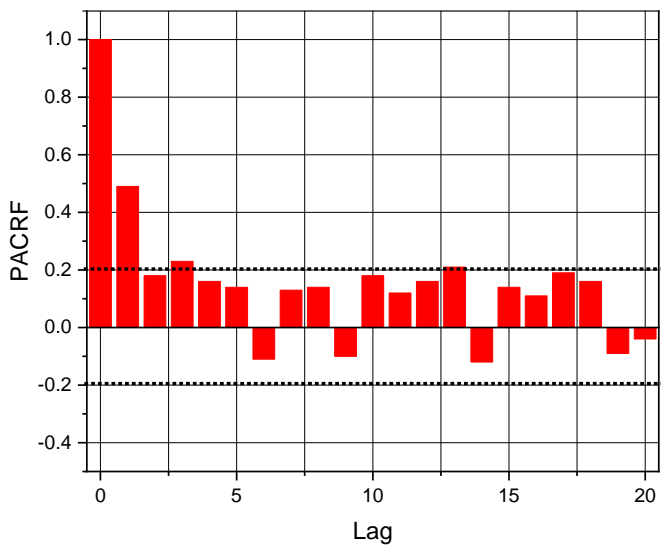


Figure 5. Variations in EI time series.



a)



b)

Figure 6. (a) ACRF variations of EI time series, (b) PACRF variations of EI time series.

On evaluating ACRF plots (Figure 6 (a)), after the first lag, the curve diminished, indicating the stationary nature. On observing PACRF plots (Figure 6 (b)), the curve diminished after a few lags. The variations were found to be with a confidence level of 95%. For satisfying the stationary time series of the Auto Regressive (AR) component, an important criterion has to be satisfied. The criterion is that, in the Partial Auto-Regressive Correlation Function (PACRF), the non-zero value should satisfy the order of the Auto Regressive (AR) model. If the criterion is not satisfied, selection of higher order is preferred for the AR model. In Box-Jenkins methodology, determination of the order of the model cannot be done, based only on PACRF variations. Hence, an appropriate criterion is necessary for selecting the order for the AR model. For estimating the prediction error, Akaike information criterion [42] was found to be better suited for this investigation as compared to Bayesian Information Criterion which requires a specific Bayesian setup [29]. Akaike information criterion helps in estimating the relative distance between the fitted and unknown likelihood function of a model. For choosing the optimal order for the AR model, Akaike Information Criterion (AIC) was used. The expression for AIC is given below

$$AIC = \log(v) + \frac{2m}{N} \quad (26)$$

In the above equation $m=a+b$ and the likelihood function is indicated as v . The calculated AIC for various orders of the model are shown in Figure 7.

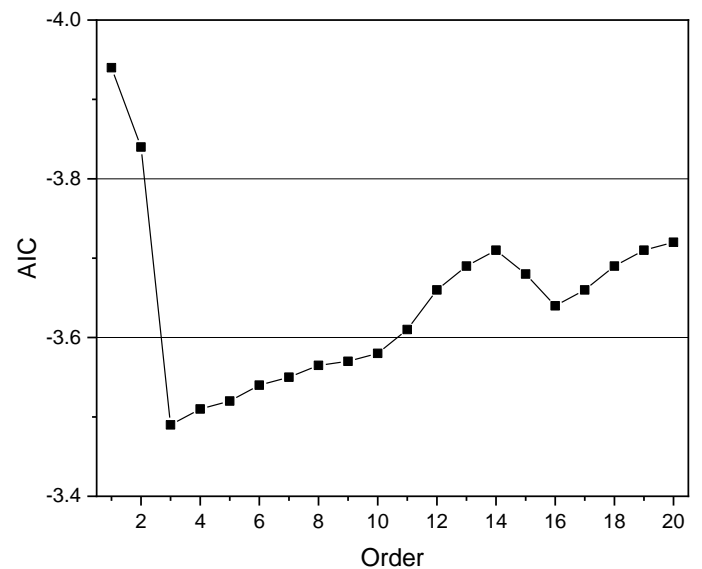


Figure 7. AIC values for various order of the model.

Many ARMA (a,b) models were evaluated for identifying

the ideal model. From Figure 7, when the order was 3, AIC value reached the minimum value and then increased on increasing the order of the model. Hence, for core drill rig performance, the ideal model selected was ARMA (3, 0). The values the model parameters (P-value, Estimate, Standard Error and t-Static) are shown in Table 2.

Table 2. Parameters of ARMA(3,0) model.

Parameter	P-Value	Estimate	Standard Error	t-Static
ARMA(1)	0.0021	0.3654	0.0412	7.31
ARMA(2)	0.1402	0.1924	0.0395	2.54
ARMA(3)	0.0001	0.0687	0.0362	1.84

Before choosing a model and estimating its parameters, the residues are subjected to diagnostic testing for verifying if the model fits with the data-series. By conducting diagnostic test, it was verified if the residuals of the chosen model from ACRF and PACRF plots were independent and normally distributed. ACRF and PARCF plots of ARMA (3, 0) residuals are shown in Figure 8 (a) and Figure 8 (b), respectively.

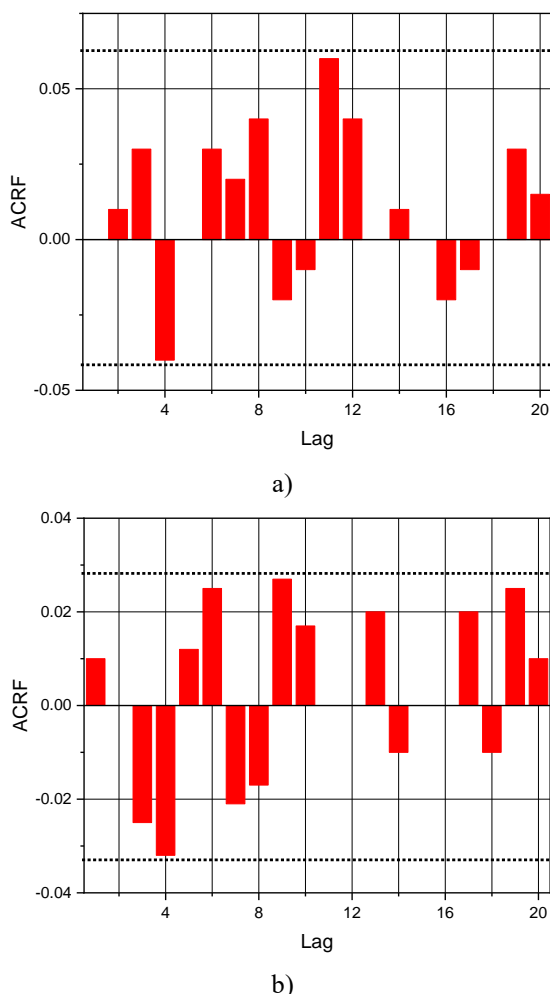


Figure 8. (a) ACRF plots for ARMA (3,0) residuals, (b) PACRF plots for ARMA(3,0).

On evaluating the peaks of ARMA (3, 0) residuals in ACRF plots (Figure 8 (a)) and in PACRF plots (Figure 8 (b)), it was found within the confidence level of 95% (upper and lower boundaries). From this evaluation, it was found that the residuals of the models were not correlated. The developed ARMA (3, 0) model was subjected to Ljung-box evaluation and the results are shown in Table 3. From Table 3, it was observed that for all lags, the value of Q-static was lesser than χ^2 value and “p-value” was greater than 0.05. It indicates that the test was insignificant and the residuals are not correlated. The non-correlation looks like random white noise. The scatter plot indicating the relationship between the observed and estimated OEE of the drill rigs are shown in Figure 9. The correlation factor (R^2) value of the scatter was found to be 0.724.

Table 3. Ljung-box test results for ARMA (3, 0) model.

Parameter	Lag (k)			
	12	24	36	48
Degree of Freedom	10	20	32	46
Q-static	8.9	24.5	36.2	39.8
Chi square	20.8	34.6	51.3	64.8
p-value	0.564	0.291	0.336	0.427

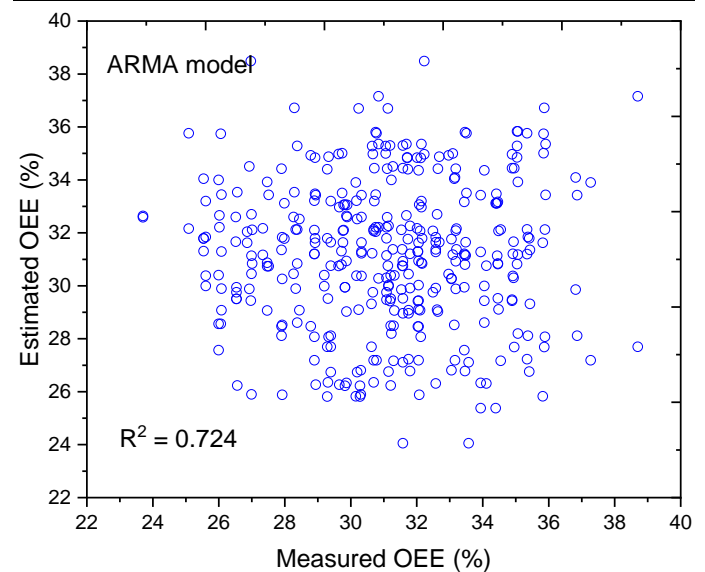


Figure 9. Correlation between measured and estimated OEE according to ARMA (3, 0) model.

A three layered non-linear autoregressive neural network (NLARNN) model was developed with MLP for estimating the effectiveness index (EI), using feed forward back propagation learning method. For attaining best prediction results, empirical studies indicated that 70 to 80% of the collected data should be used for training and 20 to 30% of the collected data should be used for testing [86]. Out of the collected data 75% was used for

training and 25% was used for testing. According to the number of lagged observations, the number of input neurons was identified. This was determined according to PACRF values [103]. By analyzing PACRF plots from Figure 6 (b), the delay was identified as 3. This was considered as input to the neurons in MLP. Using prediction accuracy indicators, the performance of the individual process parameters such as Overall Maintenance Index (OMI), Pushing Pressure (PP) in bar, Rotational Pressure (RP) in bar, Penetration Rate (PR) in m/min, Idle Time (IT) in hrs, Operated Time (OT) in hrs, Average Pillar Drill Pit Cycle Time (APDPCT) in mins, Average Time to Pillar Drill One Face Hole (ATPDFH), Average Time for Drilling One Stope Hole (ATDSH) in mins, Mean Time Before Failure (MTBF) in hrs and Productive Time (PT) in hrs were identified and the results are shown in Table 4. An incremental progressive method was used for identifying the best combination of inputs for predicting OEE. After conducting a number of trials, network with 3 inputs, one hidden layer with four neurons and one output was chosen for NLARNN model comprising PP, PR & APDPCT. The scatter diagram between the estimated and observed OEE values for NLARNN model is shown in Figure 10. Compared to ARMA (3, 0) model, the R^2 value of NLARNN model was found to be 0.812. Compared to ARMA model, a significant improvement was identified in NLARNN model.

Table 4. Performance indicator values for the individual parameters.

S No	I/p variables	Performance Indicator values					
		MAPE (%)	RMSE (%)	n-RMSE	MBE (%)	n-MBE	R^2 (%)
1	PP	22.36	31.46	0.029	1.42	0.00251	78.84
2	RP	36.89	28.64	0.027	-1.41	-0.00142	63.22
3	PR	34.31	46.45	0.031	1.83	-0.00274	76.29
4	OMI	39.24	31.26	0.058	-0.48	-0.00587	59.42
5	IT	31.08	42.64	0.069	3.12	0.00452	46.41
6	OT	34.81	28.33	0.084	1.33	0.00544	49.64
7	APDPCT	38.42	29.57	0.028	1.86	0.00219	77.49
8	ATPDFH	29.89	35.21	0.019	0.94	0.00195	69.17
9	ATDSH	32.08	31.72	0.022	-0.27	-0.00211	69.29
10	MTBF	39.28	28.79	0.065	3.03	0.00346	51.29
11	PT	63.84	32.54	0.071	2.06	0.00412	56.42

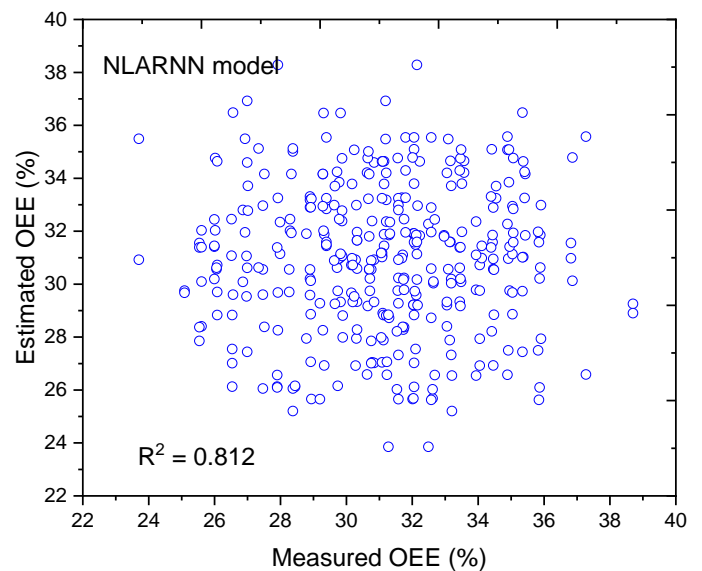


Figure 10. Correlation between measured and estimated OEE according to NLARNN model.

For building the combined hybrid model, the residuals of ARMA model was used as inputs to the new MLP model. Levenberg-Marquardt method was used for training the new combined hybrid model. Normalization of the inputs was done within the range of 0 and 1. The combined hybrid model was developed to utilize the characteristics of both ARMA model and NLARNN model. The correlations between the estimated and observed OEE values are shown in Figure 11. The R^2 value for the model was found to be 0.923.

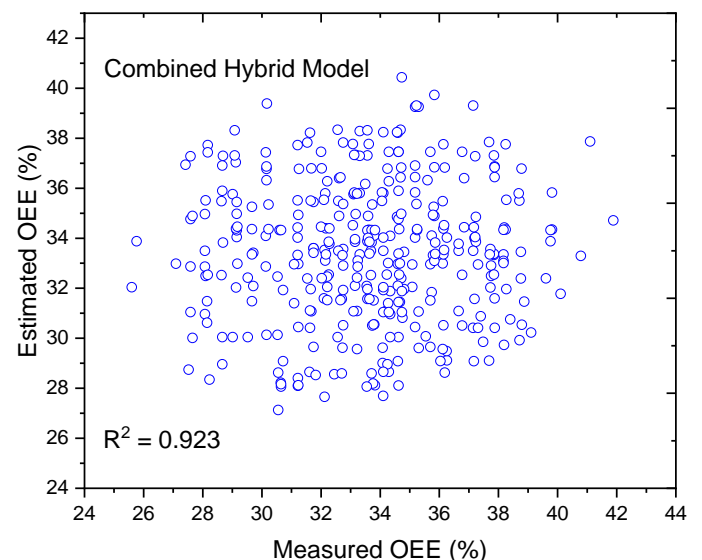


Figure 11. Correlation between measured and estimated OEE according to combined hybrid model.

As the value of R^2 was greater than the R^2 value of ARMA and NLARNN model, the predictability of the combined hybrid model was attributed to be very high. Using statistical

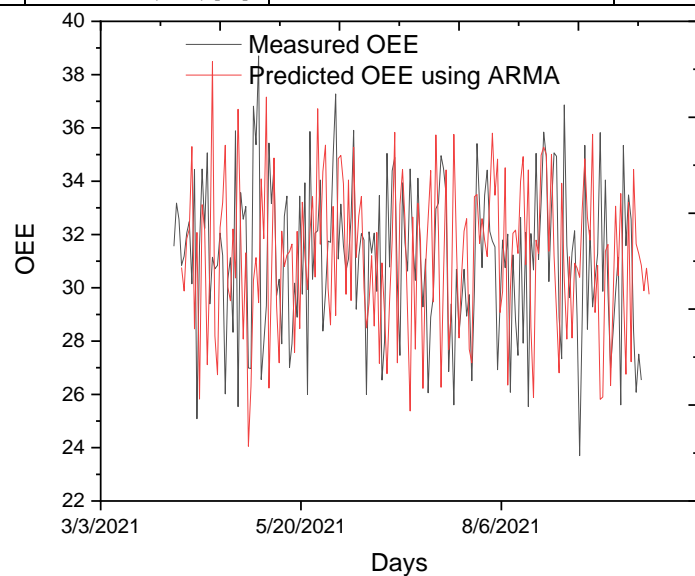
prediction accuracy indicators, the predicted OEE from ARMA, NLARNN and combined hybrid models were determined and are shown in Table 5. From Table 5, it was found that the predicted data was not in agreement with the measured values. The data predicted using NLARNN was acceptable. Comparing the prediction accuracies of ARMA and NLARNN models, the prediction accuracies of the combined hybrid model was very high. The scatter plot between the predicted and measured OEE values for ARMA, NLARNN and combined hybrid model are shown in Figure 12 (a), Figure 12 (b) and Figure 12 (c), respectively. The prediction accuracy of this method was compared with other AI based estimations conducted by other researchers. The R^2 values obtained by different models are compared in Table 6.

Table 5. Prediction accuracy indicators of the different models

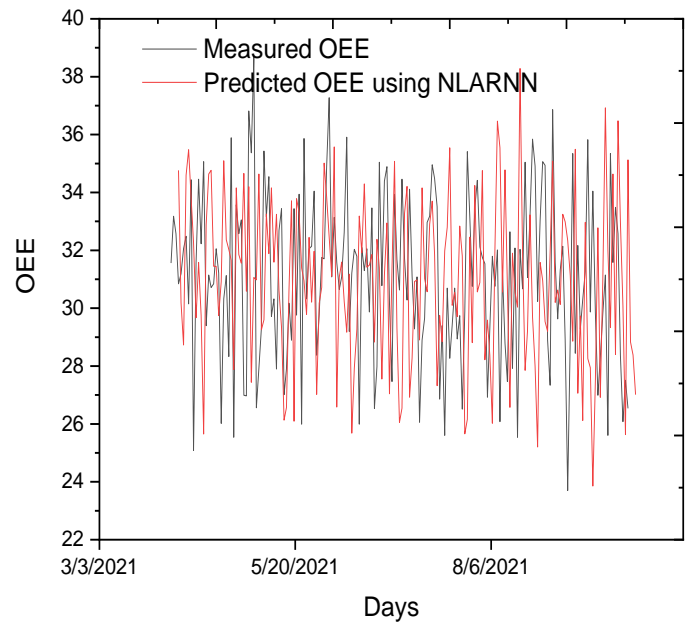
Models	Performance Indicator values					R^2
	MAPE (%)	RMSE (%)	n-RMSE (%)	MBE (%)	n-MBE (%)	
ARMA	18.321	26.419	0.241	1.69	0.0024	0.724
NLARNN	12.415	21.854	0.215	1.32	0.0021	0.812
Combined Hybrid	9.642	17.387	0.194	0.96	0.0014	0.923

Table 6. Comparison of the present hybrid model with other AI based models.

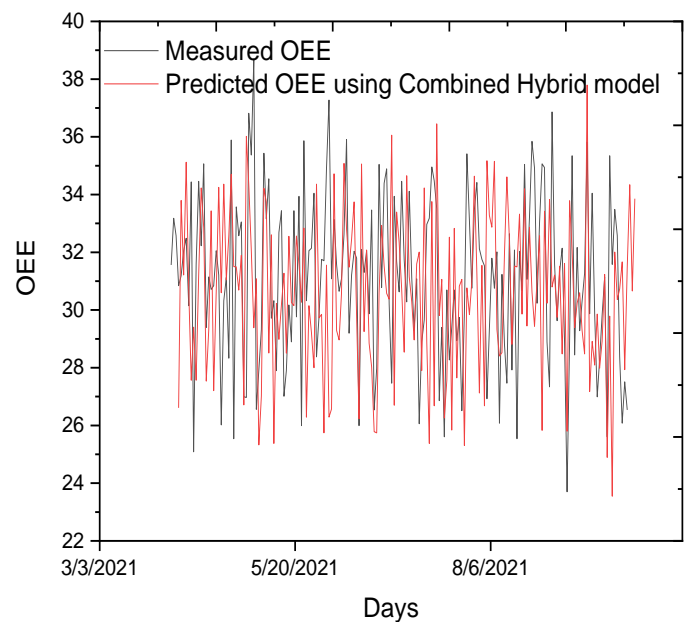
	Investigators	Models	R^2
1	Present Study	Combined ARMA- NLARNN	0.923
2	Marey et al. (2020) [63]	Feed forward ANNs and error-back propagation	0.8467
3	Hajihassani et al. (2015) [36]	ANN-Particle Swarm Optimization	0.88
4	Faradonbeh and Monjezi (2017) [23]	Cuckoo Optimization Algorithm – Gene Expression Programming	0.874
5	Sheykhi et al. (2018) [87]	Fuzzy C-Means Clustering – Support Vector Regression	0.853
6	Patraa et al. (2016) [73]	ANN	0.648



a)



b)



c)

Figure 12. Plot of obtained OEE values over predicted OEE values by (a) ARMA (3,0) model, (b) NLARNN model, (c) Combined Hybrid model.

From Figure 12, it was found that precision of the combined hybrid model was better than other two models. Hence ANN model with three parameters such as PP, PR & APDPCT were considered for optimization. From this evaluation, the decision hierarchy diagram developed for the OEE prediction model is shown in Figure 13.

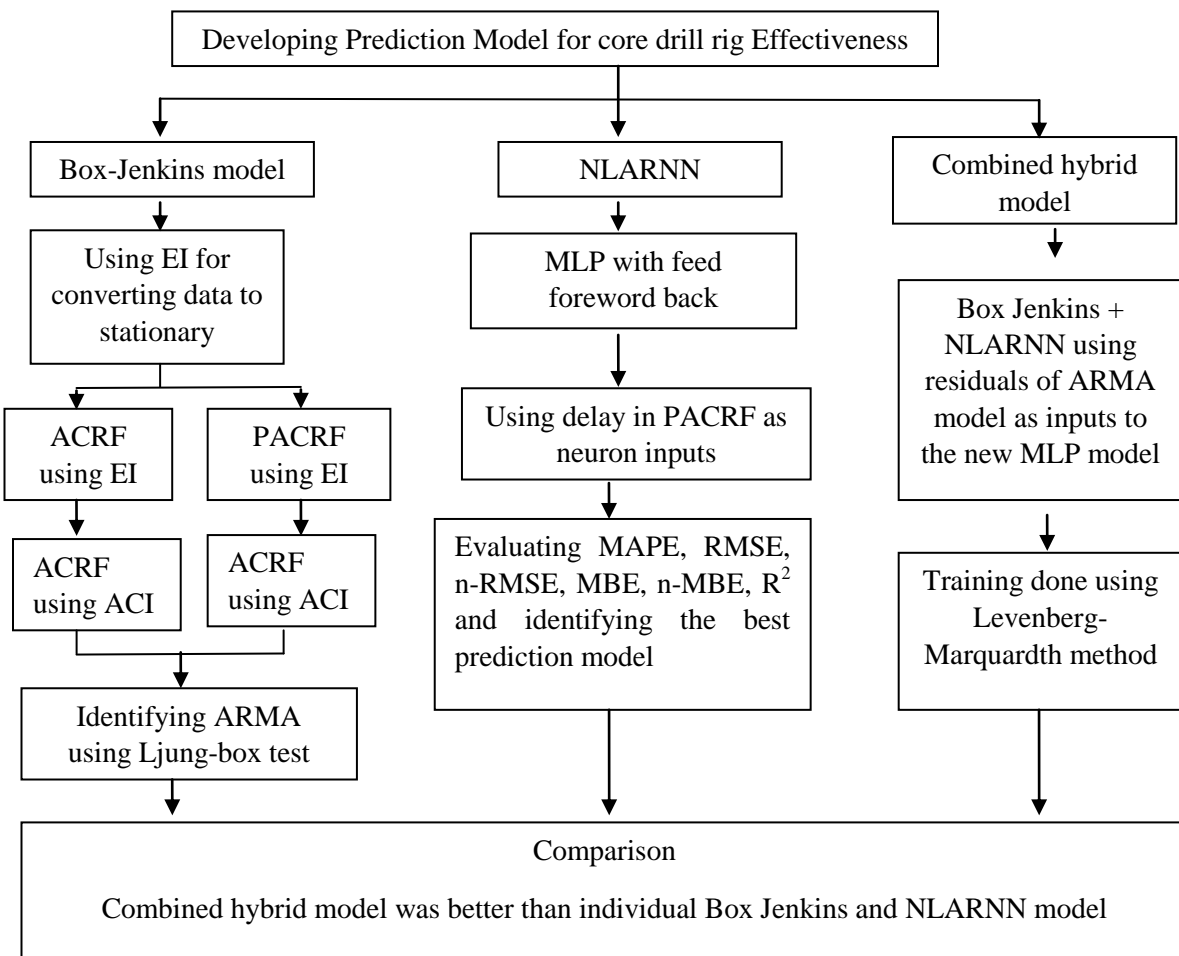


Figure 13. Decision hierarchy for the OEE prediction model.

3.2. Optimizing the core drill process parameters by using Response Surface Methodology.

In core drilling process, for accurate control over the running time, improving production and utilization, three important factors such as Pushing Pressure (PP), Penetration Rate (PR) & Average Pillar Drill Pit Cycle Time (APDPCT) were found to be important. Hence, in this investigation an attempt was made to improve OEE by optimizing PP, PR & APDPCT.

3.2.1. Identifying feasible core drill rig parameters

Using the optimized values of the three factors, availability, utilization rate and production efficiency were evaluated and from that OEE was found. Other core drilling process parameters were maintained constant within the permissible range. On conducting experimental trials, the following observations were recorded.

- a. On conducting core drilling experiments with pushing pressure less than 30 bar, the operation was more of abrasive protrusion. It resulted in excessive wear of the

drill surfaces and damaged the outer components.

- b. On conducting core drilling experiments with pushing pressure greater than 120 bar, damage to the drill rigs were more due to impulsive contact between the drilling region and the drill bit. Erosive wear was excessive leading to equipment damages.
- c. On conducting core drilling experiments with penetration rate lesser than 0.5 m/min, the drilling operation was very slow. This caused the drill bits to get heated up. Heat wear caused more damage to the equipment parts and fuel consumption was more.
- d. On conducting core drilling experiments with penetration rate greater than 2.5 m/min frequent drill bit damages were observed. It caused a lot of labor and cost to replace or service and reuse the drilling equipments.
- e. On conducting core drilling experiments with average pillar drill pit cycle time lesser than 80 mins, setup time was not sufficient to handle the vibrations induced

during drilling. Quick drilling often resulted in equipment malfunction and damage.

- f. On conducting core drilling experiments with average pillar drill pit cycle time greater than 320 mins, slow drilling was observed. This drastically reduced the production efficiency.

Hence, it was observed that within pushing pressure from 30 bar to 120 bar, drill penetration rate from 0.5 m/min to 2.5 m/min and APDPCT from 80 mins to 120 mins, functioning of the core drill rigs were feasible.

3.2.2. Developing central composite design model

For further evaluation, the three important core drilling process parameters such as PP, PR & APDPCT were used to identify OEE. The feasible limits of the core drilling process parameters are shown in Table 7.

Table 7. - Values of core drilling process parameters.

No	Parameters	Unit	Level				
			-1.682	-1.0	0	+1.0	+1.682
1	PP	Bar	30	50	75	100	120
2	PR	m/min	0.5	0.9	1.5	2	2.5
3	APDPCT	mins	80	130	200	270	320

For optimizing, a central composite design model was developed with five levels. The lower most variable was assigned as -1.682 and the upper moat variable was assigned as +1.682. The intermediate values were identified according to the equation developed by Montgomery [67]

$$B_i = 1.682 [2B - (B_{max} + B_{min})] \div (B_{max} + B_{min}) \quad (27)$$

In the above equation, B is assigned values from B_{min} to B_{max} . B_{max} is the maximum value, a variable can be assigned and B_{min} is the minimum value, a variable can be assigned. The intermediate values are ere .calculated and are shown in Table 7. The central composite design developed for core drill rig performance improvement model is shown in Table 8.

Table 8. Central composite design model for core drill rig performance enhancement model.

Sl. No.	Coded Factor value			Actual Factor value			Responses (OEE)
	PP	PR	APDPCT	PP (bar)	PR (m/min)	APDPCT (min)	OEE (%)
1	0	0	0	75	1.50	200	72.71
2	0	-1.682	0	75	0.50	200	68.86
3	+1	-1	+1	100	0.90	270	74.98
4	-1	+1	+1	50	2.0	270	71.31
5	0	+1.682	0	75	2.5	200	71.31
6	+1	+1	-1	100	2.0	130	69.38
7	0	0	0	75	1.5	200	72.81
8	-1	-1	-1	50	0.90	130	64.13
9	-1.682	0	0	30	1.5	200	69.38
10	-1	-1	+1	50	0.90	270	69.31
11	-1	+1	-1	50	2.0	130	71.92
12	+1	-1	-1	100	0.90	130	68.42
13	0	0	0	75	1.5	200	72.88
14	+1	0+1	+1	100	2.0	270	70.52
15	0	0	0	75	1.5	200	72.36
16	0	0	-1.682	75	1.5	80	67.37
17	0	0	+1.682	75	1.5	320	72.27
18	0	0	0	75	1.5	200	72.715
19	+1.682	0	0	120	1.5	200	72.01
20	0	0	0	75	1.5	200	72.62

With the values of the process parameters indicated in the design model core drilling experiments were conducted and the relevant A, UR and PR were identified. Using the values, OEE

was calculated and recorded in Table 8. Six repetitive experiments were used to eliminate errors. The standard error of the developed design is shown in Figure 14.

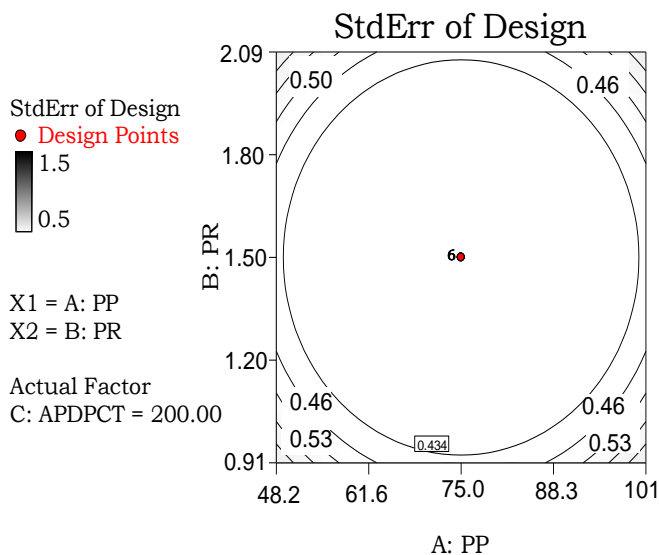


Figure 14. Standard error of the core drill rig performance improvement model.

3.2.3. Developing empirical equations between core drill rig process parameters and OEE

The output response in the form of OEE was attributed to be a function of the three core drill rig process parameters such as PP, PR and APDPCT. According to the relationship developed by Paventhan et al. (2012) [72], the following equation was developed

$$OEE = f(PP, PR, APDPCT) \quad (28)$$

The response surface (RS) of the core drill rig performance enhancement model has been indicated as second order regression equation as follows

$$RS = g_0 + \sum g_i w_i + \sum g_{i1} w_{i2} + \sum g_{ij} w_i w_j \quad (29)$$

For three input variables such as PP, PR and APDPCT, the second order regression equation is shown as follows

$$OEE = \{w_0 + w_1(PP) + w_2(PR) + w_3(APDPCT) + w_{12}(PP \times PR) + w_{13}(PP \times APDPCT) + w_{23}(PR \times APDPCT) + w_{11}PP^2 + w_{22}PR^2 + w_{33}APDPCT^2\} \quad (30)$$

In Eq. 29 and Eq. 30, g_0 is termed as the average of response (OEE). The coefficients of the regression equations are $g_1, g_2, g_3, \dots, g_n$. These coefficients depend on the linear, square and interaction terms. The coefficients were evaluated by Design Expert. Student t tests and p values were used for evaluating the values of individual coefficients. Using Mann Whitney U test, the Z-score value was identified as -0.1488 and the other important results of Mann Whitney U test are shown in Table 9.

Table 9. Results of Mann Whitney U test.

	N	Min	Median	Max	Mean Rank	Sum Rank
Predicted OEE	20	64.137	71.61875	74.9875	20.2	404
Actual OEE	20	64.144	71.62499	74.9965	20.8	416
Test Statistics						
U					194	
Z					-0.1488	
Asymp. Prob> U					0.88171	

On evaluating the model at 0.05 level, there were no significant difference in distribution of the two. Hence, from Mann Whitney U test analysis, a very close relationship between the predicted and actual values of OEE was ascertained. The significance of the developed model was ascertained using type III analysis of variance. The analysis of variance results of the core drill rig performance improvement model is shown in Table 10.

Table 10. Analysis of variance results of core drill rig performance improvement model.

Source	Sum of Squares (SS)	Degree of freedom (df)	Mean square (MS)	F - ratio	p-value Prob>F	Note
Model	113.86	9	12.49	581.39	<0.0001	Significant
PP	8.41	1	8.41	363.48	<0.0001	
PR	7.39	1	7.39	348.62	<0.0001	
APDPCT	31.24	1	31.24	1344.02	<0.0001	
PP x PR	21.46	1	21.46	982.31	<0.0001	
PP x APDPCT	1.08	1	1.08	53.54	<0.0001	
PR x APDPCT	13.62	1	13.62	699.59	<0.0001	
PP ²	7.41	1	7.41	334.17	<0.0001	
PR ²	13.36	1	13.36	246.41	<0.0001	
APDPCT ²	14.48	1	14.48	375.69	<0.0001	
Residual	0.26	10	0.017			

Source	Sum of Squares (SS)	Degree of freedom (df)	Mean square (MS)	F - ratio	p-value Prob>F	Note
Lack of fit	0.042	5	0.008		0.8635	Not significant
Std. Dev		0.13		R ²	0.9853	
Mean		71.25		Adj	0.9854	
C.V. %		0.23		Pred	0.9795	
PRESS		0.71		Adeq precision	101.024	

Using ANOVA, sum of squares, mean square, F-ratio and p-values for PP, PR, APDPCT, PP x PR, PP x APDPCT, PR x APDPCT, PP², PR² and APDPCT² were evaluated. The value of sum of squares and F-ratio of the model was found to be 113.86 and 581.39 respectively. From the value of F-ratio, it was inferred that the developed core drill rig performance improvement model was significant. As the “Prob>F” values were lower than 0.0001, the model was significant. Lack of fit was insignificant as its value was 0.8635. As the value of R², Adjusted R² and predicted R² values were 0.9853, 0.9854 and 0.9795, the significance of the developed model was ascertained to be very high. The empirical equation developed for establishing the relationship between the input and out values are shown below

$$OEE = \{+26.18 + 0.29(PP) + 23.60(PR) + 0.13(APDPCT) - 0.104(PP \times PR) + 2.06(PP \times APDPCT) - 0.03(PR \times APDPCT) - 9.95PP^2 - 2.62PR^2 - 2.07APDPCT^2\} \quad (31)$$

The scatter diagram indicating the correlation between the actual and predicted OEE is shown in Figure 15. On studying the scatter graph, a high level of correlation was observed with the predicted and actual values.

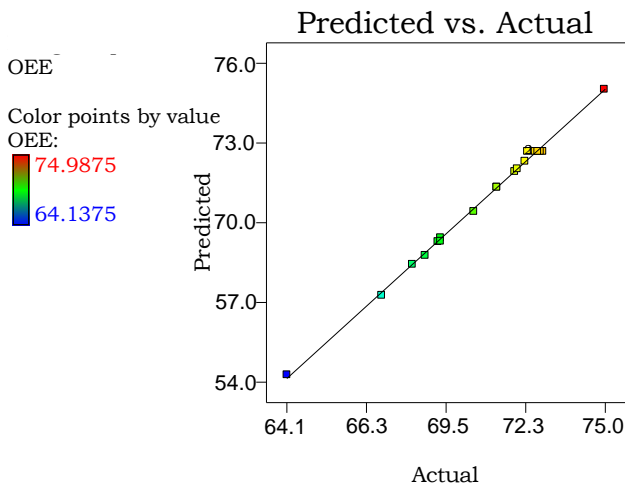


Figure 15. Scatter plot of predicted and actual OEE values.

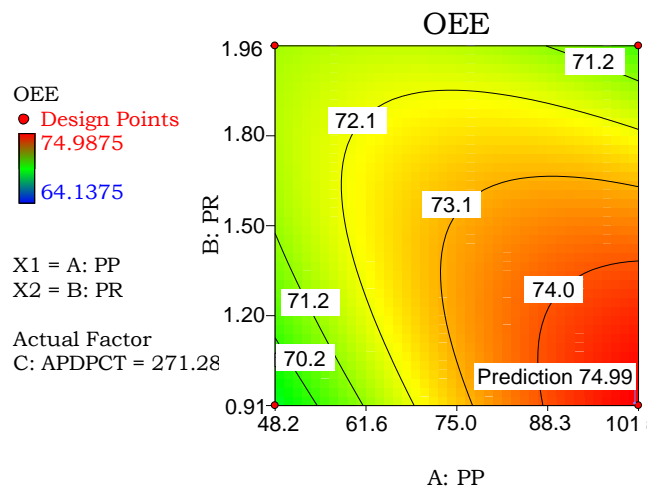
3.2.4 Optimizing core drilling process parameters using response surface methodology

Using response surface methodology, the important core drilling process parameters such as PP, PR and APDPCT were optimized. The goal of this optimization method is to improve OEE of core drill rig to the maximum possible limit. The response surface equation for optimization is given below

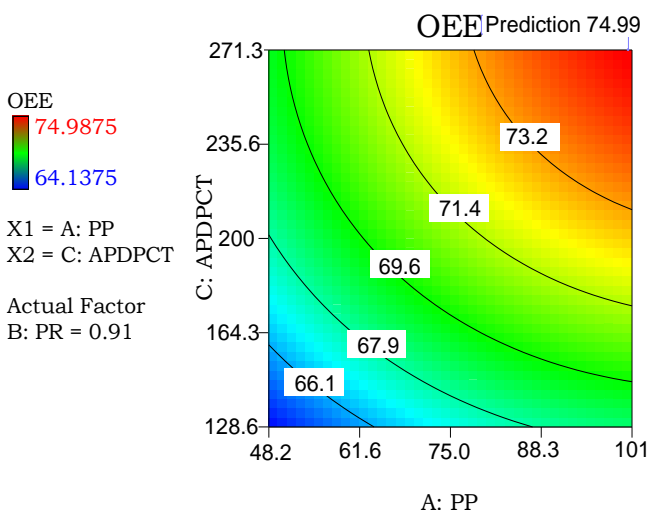
$$R = \Phi(u_1, u_2 \dots u_k) \pm er. \quad (32)$$

In Eq. 29, the response is indicated as R, residual error is denoted as er and the quantitative factors are denoted as u₁, u₂ ... u_k. For predicting OEE, a characteristic surface was developed using the independent variables. Response surface was prepared by varying the values of the process parameters from -1.682 to +1.682. The developed surface was fitted into regression equations. Contours were developed using two of the process variables and keeping the third as constant. The changes in output response (OEE) were plotted with varying the two process parameters. From the developed contours, the optimal area was identified. Simple contours can be created using first order equations. On increasing the complexity of contours, the order of the equations increases. Within the optimal surface region, the stationary point was observed. The stationary point was identified as saddle, maximum or minimum. Using design expert software, contour plots were developed. Circular shapes of contours indicate that there is no interaction between the independent factors. Elliptical shapes of contours indicate interactions. 3-D surface plots were developed by using two of the input process parameters while maintaining the third as constant. The shape of the 3-D surface plots was evaluated and the optimum region was identified. Using Design Expert, 3-D surface plots were developed, compared with the contours to identify the optimized core drill rig process parameters. The developed contour plots are shown in Figure 16. Contour plot of PP vs PR at constant APDPCT of 271.28 mins is shown in

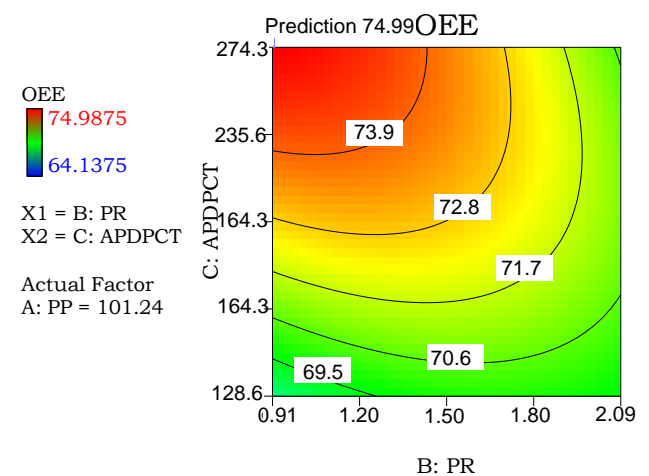
Figure 16 (a). Contour plot of PP vs APDPCT at constant PR of 0.91 m/min is shown in Figure 16 (b). Contour plot of PR vs APDPCT at constant PP of 101.24 bar is shown in Figure 16 (c).



a) Contour plot for PP vs PR.



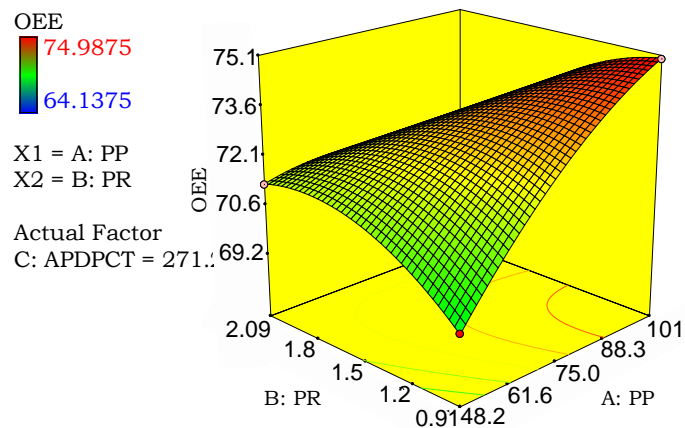
b) Contour plot of PP vs APDPCT.



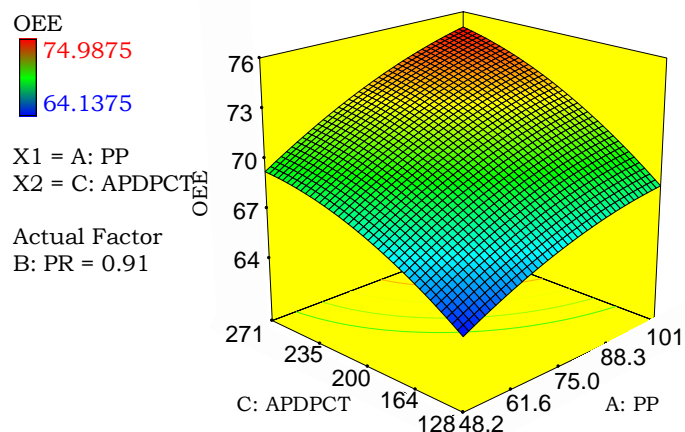
c) Contour plot of PR vs APDPCT

Figure 16. Contour plots of core drill rig parameters optimization model.

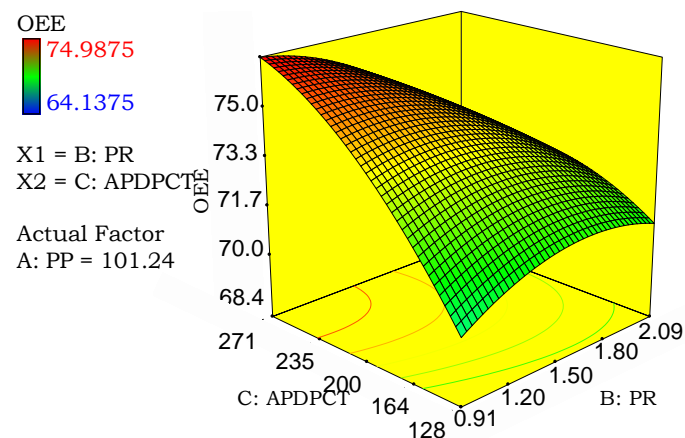
The developed 3-D surface plots are shown in Figure 17. 3-D surface plot of PP vs PR at constant APDPCT of 271.28 mins is shown in Figure 17 (a). 3-D surface plot of PP vs APDPCT at constant PR of 0.91 m/min is shown in Figure 17 (b). 3-D surface plot of PR vs APDPCT at constant PP of 101.24 bar is shown in Figure 17 (c).



a) 3D surface plot of PP vs PR



b) 3D surface plot of PP vs APDPCT.



c) 3D surface plot of PR vs APDPCT.

Figure 17. 3-D surface plots of core drill rig parameters optimization model.

On evaluating the developed contours and 3-D surface plots, the maximum possible OEE was predicted to be 74.99 %. The corresponding predicted core drill rig process parameters were pushing pressure of 101.7 bar, penetration rate of 0.94 m/min and average pillar drill pit cycle time of 272 min. For validation of the optimization model, validation experiments were conducted. Three experiments were conducted with the optimized values of process parameters and the corresponding OEE was calculated. The difference between the predicted and actual vales of OEE was calculated and recorded in Table 11. From validation experiments, it was found that the error between the predicted and actual values were lesser than 5%. This indicated that the model was developed with very high accuracy.

Table 11. Results of validation experiments.

Exp No	OEE of core drill rigs		Error %
	Predicted OEE (%)	Experimental OEE (%)	
1	74.99	73.41	-2.10
2		72.96	-2.70
3		71.89	-4.13

3.2.5 Interactions, perturbation and sensitivity analysis

Interaction plots are used for identifying the dependence of one variable with another in multi criteria optimization models. Perturbation plots are used for identifying the effect of all input factors in a system on the response within the design space [58]. Sensitivity analysis is used to identify the most important input variable affecting the output response in a design model [45]. Interactions between the three input variables of the core drill rigs such as pushing pressure, drill penetration rate and average pillar drill pit cycle time were identified by developing interaction plots. The effect of variations in two of the drill rig process parameters and the corresponding changes in OEE was plotted. The interaction plots are shown in Figure 18. Interaction plots between PP and PR against OEE at constant APDPCT of 270.10 is shown in Figure 18 (a). Interactions were observed at lower side of the feasible range. Interaction plots between PP and APDPCT against OEE at constant PR of 2.0 m/min is shown in Figure 18 (b). Interactions were observed at the lowermost edge of feasible range. Interaction plots between PR and APDPCT against OEE at constant PP of 53.31 bar is shown in Figure 18 (c). Interactions were observed at upper side of the feasible range.

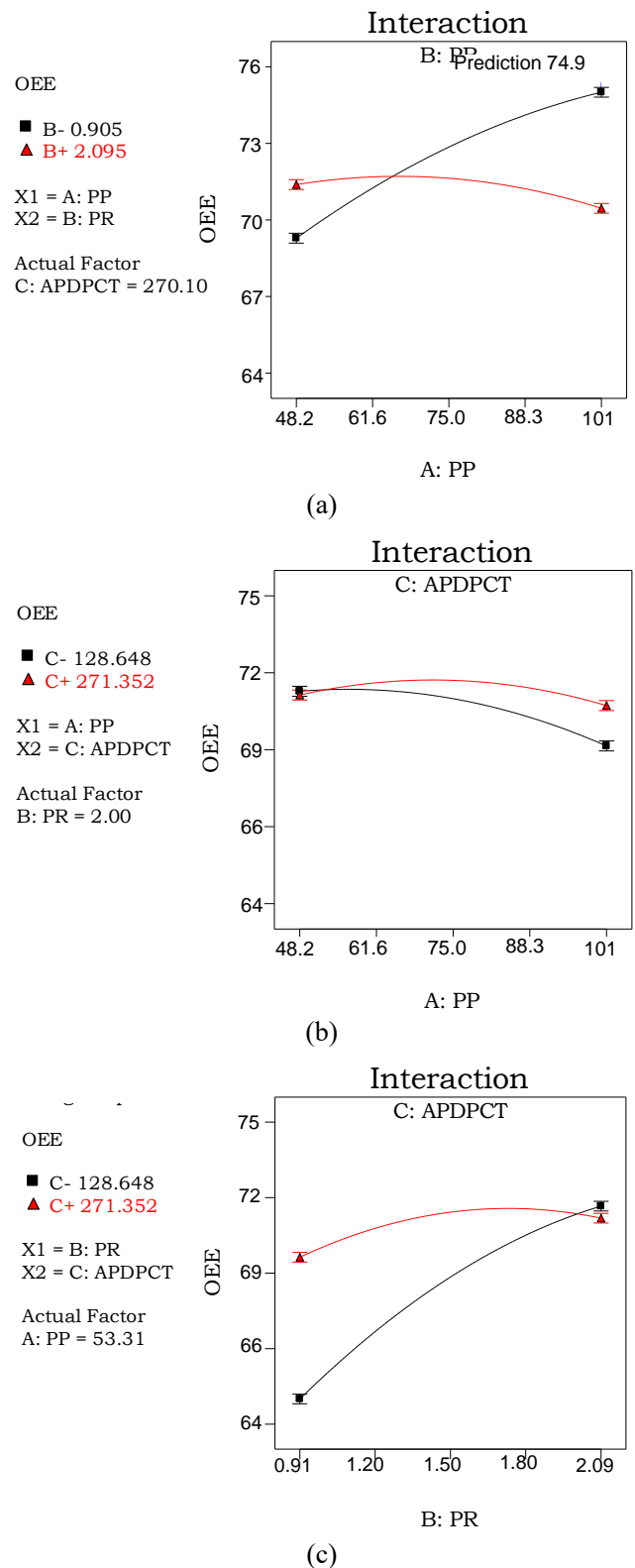


Figure 18. Interaction plots between core drill parameters on OEE.

Perturbation plots were developed at PP of 75.72 bar, PR of 1.37 m/min and APDPCT of 201.9 min and is shown in Figure 19. OEE variations were identified on increasing and decreasing the core drill process parameters. On studying the perturbation plots, it was observed that APDPCT variations had a greater

effect on OEE, than the other two core drilling process parameters.

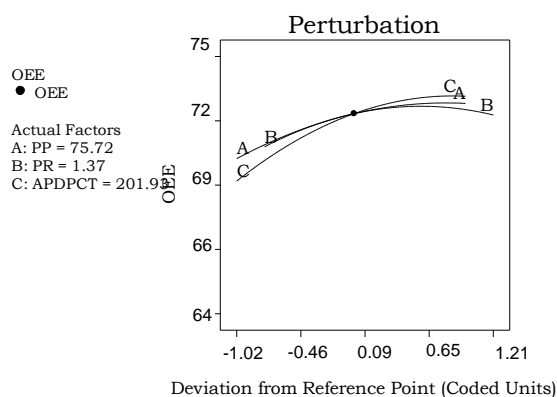


Figure 19. Perturbation plots of core drill process parameters.

For ranking the process parameters, sensitivity analysis was conducted. Sensitivity equations were prepared by partial differentiation of the developed empirical equations w.r.t. the core drilling parameters. The developed empirical equations are shown as follows

$$dOEE/dPP = \{0.29 - 919.9PP - 0.104PR + 2.06APDPCT\} \quad (33)$$

$$dOEE/dPR = \{+23.60 - 0.104PP - 5.24PR - 0.04APDPCT\} \quad (34)$$

$$dOEE/dAPDPCT = \{+0.13 + 2.06PP - 0.03PR - 4.14APDPCT\} \quad (35)$$

The equations were used to construct sensitivity graphs, on substituting the process parameter values in the sensitivity equations. The sensitivity values of the partially differentiated OEE w.r.t. PP, PR and APDPCT are shown in Table 12.

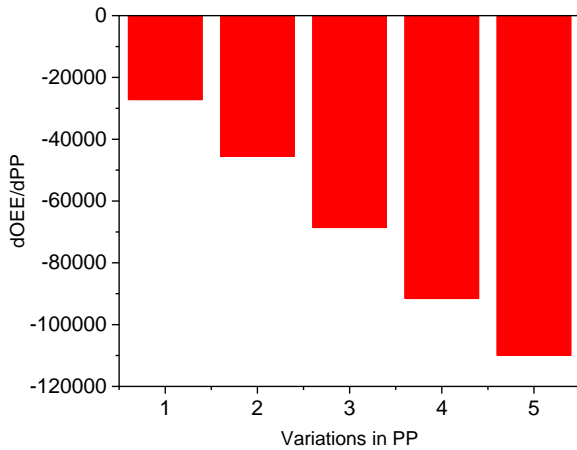
Table 12. Sensitivity values of the developed OEE improvement model.

S No	PP	PR	APDPCT	dOEE/dPP	dOEE/dPR	dOEE/dAPDPCT
1	30	0.5	80	-27431.9	14.02	-269.285
2	50	0.9	80	-45830.0	9.844	-228.097
3	75	1.5	80	-68827.5	4.1	-176.615
4	100	2	80	-91825.1	-1.12	-125.13
5	120	2.5	80	-110223.1	-5.82	-83.945
6	30	0.5	130	-27328.9	11.62	-476.285
7	50	0.9	130	-45727.0	7.444	-435.097
8	75	1.5	130	-68724.5	1.7	-383.615
9	100	2	130	-91722.1	-3.52	-332.13
10	120	2.5	130	-110120.7	-8.22	-290.945
11	30	0.5	200	-27184.7	8.26	-766.085
12	50	0.9	200	-45582.8	4.084	-724.897
13	75	1.5	200	-68580.3	-1.66	-673.415
14	100	2	200	-91577.9	-6.88	-621.93
15	120	2.5	200	-109975.0	-11.58	-580.745
16	30	0.5	270	-27040.5	4.9	-1055.885
17	50	0.9	270	-45438.6	0.724	-1014.697
18	75	1.5	270	-68436.1	-5.02	-963.215
19	100	2	270	-91433.7	-10.24	-911.73
20	120	2.5	270	-109831.7	-14.94	-870.545
21	30	0.5	320	-26937.5	2.5	-1262.885
22	50	0.9	320	-45335.6	-1.676	-1221.697
23	75	1.5	320	-68333.1	-7.42	-1170.215
24	100	2	320	-91330.7	-12.64	-1118.73
25	120	2.5	320	-109728.7	-17.34	-1077.545

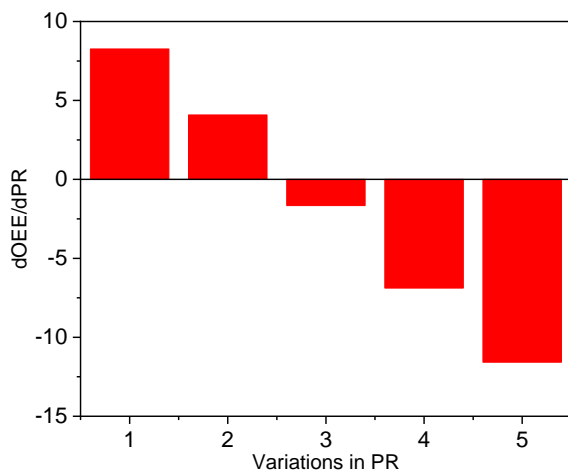
From the sensitivity values, sensitivity graphs were developed and are shown in Figure 20. Graph for variations in sensitivity on OEE for variations in PP is shown in Figure 20

(a). Similarly, the sensitivity graphs for variation in sensitivity on OEE for variations in PR and APDPCT are shown in Figure 20 (b) and Figure 20 (c). Sensitivity for the output response is

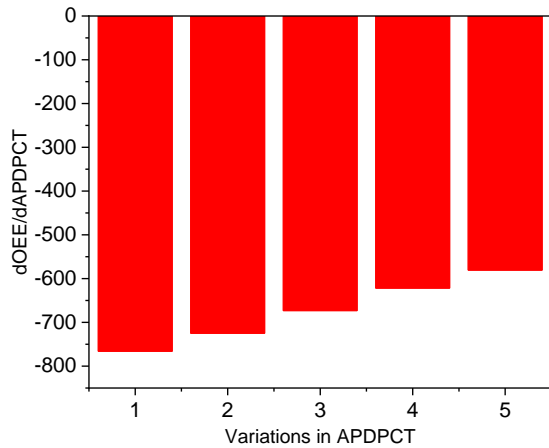
highest for that parameter, which varies the output response to the maximum extent (positive to negative or negative to positive). On evaluating the sensitivity graphs, variations in PR was found to affect the output OEE to a greater extent, compared to the variations in PP and APDPCT. Hence, a slight modification in PR affected OEE to a greater extent than PP and APDPCT.



a)



b)



c)

Figure 20. Graphs for variations in sensitivity.

The decision hierarchy for indicating the optimization model is shown in Figure 21

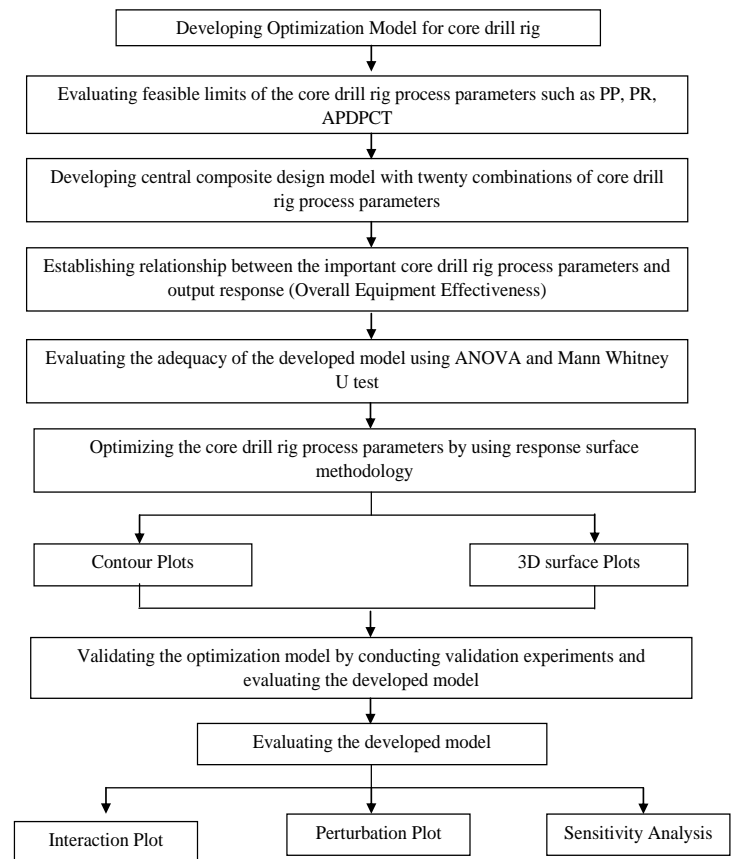


Figure 21. Decision hierarchy for the optimization model.

4. CONCLUSIONS

Hence, in this investigation an attempt was successfully made to improve the overall equipment effectiveness of core dill rig. A combined approach using Box Jenkins (Auto Regressive Moving Average) model combined with non-linear auto regressive based artificial neural network model was used for prediction. Before implementing auto-regressive moving average model, the values of overall equipment effectiveness values were modified into effectiveness index for converting it into stationary data. Statistical accuracy indicators such as coefficient of determination, root mean square error, normalized root mean square error, mean bias error, normalized mean bias error and mean average percentage error was used to ascertain the prediction accuracy of the developed models. On studying the values of prediction accuracy indicators, the accuracy of combined hybrid model was found to be better than auto regressive moving average model and non-linear auto regressive based artificial neural network model and artificial neural network model with three parameters such as PP, PR &

APDPCT were considered for optimization. Feasible limits were identified for the core drilling process parameters and central composite design model was used for conducting optimization studies. Empirical relationships were developed between the three important core drill parameters such as pushing pressure, penetration rate and average pillar drill pit cycle time and overall equipment efficiency. The significance of the empirical relationships was evaluated to a confidence level greater than 95% using analysis of variance. Using contours and

3-D surface plots, the core drilling parameters were optimized for achieving highest possible overall equipment effectiveness of 74.9%. Interactions between the process parameters were analyzed and the perturbation ranked the priority of average pillar drill pit cycle time higher than the other two parameters. Sensitivity analysis indicated that overall equipment effectiveness was more sensitive to variations in drill penetration rate than the other two process parameters.

Acknowledgement:

The authors thank the assistance rendered by M/s. Vikram Engineering Industry, Tiruchirappalli, Tamil Nadu, India for their assistance in modeling and optimization studies.

References

1. Abedi M, Norouzi GH, Bahroudi, A. Support vector machine for multi-classification of mineral prospectivity areas. *Computers & Geosciences* 2012; 46(1): 272-283, <http://dx.doi.org/10.1016/j.cageo.2011.12.014>
2. Alipour A, Mokhtarian M. RSM-based model to estimate the V-Cut drill and blast pattern specific charge in rock tunneling. *International Journal of Geomechanics* 2021; 21(11): 06021030, [http://dx.doi.org/10.1061/\(ASCE\)GM.1943-5622.0002180](http://dx.doi.org/10.1061/(ASCE)GM.1943-5622.0002180)
3. Amini E, Nasiri M, Pargoo NS, Mozhgani Z, Golbaz D, Baniesmaeil M, Nezhad MM, Neshat M, Garcia DA, Sylaios G. Design optimization of ocean renewable energy converter using a combined Bi-level metaheuristic approach. *Energy Conversion and Management: X*. 2023 Jul 1;19:100371, <https://doi.org/10.1016/j.ecmx.2023.100371>
4. Anvarovich IB, Yashnarovna IM. Predictive Models for Effective Management of E-commerce in New Uzbekistan. In *Internet of Things, Smart Spaces, and Next Generation Networks and Systems: 22nd International Conference, NEW2AN 2022, Tashkent, Uzbekistan, December 15–16, 2022, Proceedings* 2023 Apr 20 (pp. 636-648). Cham: Springer Nature Switzerland, https://doi.org/10.1007/978-3-031-30258-9_57
5. Bandyopadhyay LK, Chaulya SK, Mishra PK.. Wireless communication in underground mines. *RFID-Based Sens. Netw.* 2010, 22., <http://dx.doi.org/10.1007/978-0-387-98165-9>
6. Basarir H, Tutluoglu L, Karpuz C. Penetration rate prediction for diamond bit drilling by adaptive neuro-fuzzy inference system and multiple regressions. *Engineering Geology* 2014; 173(1): 1-9, <https://doi.org/10.1016/j.enggeo.2014.02.006>
7. Beaton T, Cyre J, Isnor S, Herman JJ. New technologies eliminate drill bit wear in oil sands applications. In *SPE Unconventional Resources Conference Canada 2013; OnePetro*, <http://dx.doi.org/10.2118/167133-MS>
8. Bevilacqua M, Ciarapica FE, De Sanctis I, Mazzuto G, Paciarotti C. A Changeover Time Reduction through an integration of lean practices: a case study from pharmaceutical sector. *Assembly Automation* 2015; 35(1): 22-34, <http://dx.doi.org/10.1108/AA-05-2014-035>
9. Bevilacqua A, Speranza B, Petrucci L, Sinigaglia M, Corbo MR. Using regression and Multifactorial Analysis of Variance to assess the effect of ascorbic, citric, and malic acids on spores and activated spores of *Alicyclobacillus acidoterrestris*. *Food Microbiology*. 2023 Apr 1;110:104158, <https://doi.org/10.1016/j.fm.2022.104158>
10. Castellon DF, Fenerci A, Øiseth O. A comparative study of wind-induced dynamic response models of long-span bridges using artificial neural networks, support vector regression and buffeting theory. *Journal of Wind Engineering and Industrial Aerodynamics* 2021; 209(1): 104484, <https://doi.org/10.1016/j.jweia.2020.104484>
11. Chaabene M, Ammar MB. Neuro-fuzzy dynamic model with Kalman filter to forecast irradiance and temperature for solar energy systems. *Renewable Energy* 2008; 33(7): 1435-1443, <http://dx.doi.org/10.1016/j.renene.2007.10.004>
12. Castellano-Méndez M, González-Manteiga W, Febrero-Bande M, Prada-Sánchez JM, Lozano-Calderón R. Modelling of the monthly and daily behaviour of the runoff of the Xallas river using Box–Jenkins and neural networks methods. *Journal of hydrology* 2004; 296(1-4): 38-58, <https://doi.org/10.1016/j.jhydrol.2004.03.011>

13. Cao X, Kozhevnykov A, Dreus A, Liu BC. Diamond core drilling process using intermittent flushing mode. *Arabian Journal of Geosciences*. 2019 Feb;12:1-7, <https://doi.org/10.1007/s12517-019-4287-2>
14. Choubin B, Malekian A. Combined gamma and M-test-based ANN and ARIMA models for groundwater fluctuation forecasting in semiarid regions. *Environmental Earth Sciences* 2017; 76(1): 1-10,, <https://doi.org/10.1007/s12665-017-6870-8>
15. Cui H, Qiu J, Cao J, Guo M, Chen X, Gorbachev S. Route optimization in township logistics distribution considering customer satisfaction based on adaptive genetic algorithm. *Mathematics and Computers in Simulation*. 2023 Feb 1;204:28-42, <http://dx.doi.org/10.1016/j.matcom.2022.05.020>
16. De Giorgi MG, Campilongo S, Ficarella A, Congedo PM. Comparison between wind power prediction models based on wavelet decomposition with least-squares support vector machine (LS-SVM) and artificial neural network (ANN). *Energies* 2014; 7(8): 5251-5272, <https://doi.org/10.3390/en7085251>
17. Deng F, Shen S, He J, Yue W, Qian K, Miao X, Xu P, Wang M. The novel characteristics for training Ridge Polynomial neural network based on Lagrange multiplier. *Alexandria Engineering Journal*. 2023 Mar 15;67:93-103, <https://doi.org/10.1016/j.aej.2022.07.017>
18. de Oliveira WB, Lisboa TP, da Silva GC, Oliveira RS, de Souza CC, Matos MA, de Oliveira MA, Matos RC. Box-Behnken Factorial Design Applied to Electrodeposition of Silver Nanoparticles in 3D-Printed Disposable Device for the Determination of Sulfamethoxazole in Different Samples by Differential Pulse Voltammetry. Available at SSRN 4436897, <https://dx.doi.org/10.2139/ssrn.4436897>
19. Ding K, Chen X, Weng S, Liu Y, Zhang J, Li Y, Yang Z. Health status evaluation of photovoltaic array based on deep belief network and Hausdorff distance. *Energy*. 2023 Jan 1;262:125539, <https://doi.org/10.1016/j.energy.2022.125539>
20. Dobra P, Jósvali J. Assembly line overall equipment effectiveness (OEE) prediction from human estimation to supervised machine learning. *Journal of Manufacturing and Materials Processing* 2022; 6(3): 59, <https://doi.org/10.3390/jmmp6030059>
21. Dodevska Z, Petrović A, Radovanović S, Delibašić B. Changing criteria weights to achieve fair VIKOR ranking: a postprocessing reranking approach. *Autonomous Agents and Multi-Agent Systems*. 2023 Jun;37(1):9, <https://doi.org/10.1007/s10458-022-09591-5>
22. Fajun Z, Qigen D, Fuchang H, Weiqin Z. A new method of coring in coal mine: pressure-holding and continuous coring technology. *Bulletin of Engineering Geology and the Environment*. 2023 Jan;82(1):17, <https://doi.org/10.1007/s10064-022-03038-7>
23. Faradonbeh RS, Monjezi M. Prediction and minimization of blast-induced ground vibration using two robust meta-heuristic algorithms. *Engineering with Computers* 2017; 33(1): 835-851, <https://doi.org/10.1007/s00366-017-0501-6>
24. Fekri Sari M, Avakh Darestani S. Fuzzy overall equipment effectiveness and line performance measurement using artificial neural network. *Journal of quality in maintenance engineering* 2019; 25(2): 340-354, <https://doi.org/10.1108/JQME-12-2017-0085>
25. Feldman R, Sanger J. *The text mining handbook: advanced approaches in analyzing unstructured data*. Cambridge university press 2007, <https://doi.org/10.1017/CBO9780511546914>
26. Fernandez-de-Cossio-Diaz J, Cocco S, Monasson R. Disentangling representations in restricted boltzmann machines without adversaries. *Physical Review X*. 2023 Apr 5;13(2):021003, <https://doi.org/10.1103/PhysRevX.13.021003>
27. Figiel A, Klačková I. Safety requirements for mining systems controlled in automatic mode. *Acta Montanistica Slovaca* 2020; 25(3), <https://doi.org/10.46544/AMS.v25i3.13>
28. Flores JHF, Engel PM, Pinto RC. Autocorrelation and partial autocorrelation functions to improve neural networks models on univariate time series forecasting. In *The 2012 International Joint Conference on Neural Networks (IJCNN) 2012*; 1-8, <http://dx.doi.org/10.1109/IJCNN.2012.6252470>
29. Follett L, Vander Naald B. Heterogeneity in choice experiment data: A Bayesian investigation. *Journal of Choice Modelling*. 2023 Jan 4:100398, <https://doi.org/10.1016/j.jocm.2022.100398>
30. Fonseca, D.J., Navarrese, D.O. and Moynihan, G.P., 2003. Simulation metamodeling through artificial neural networks. *Engineering applications of artificial intelligence*, 16(3), pp.177-183. [https://doi.org/10.1016/S0952-1976\(03\)00043-5](https://doi.org/10.1016/S0952-1976(03)00043-5)
31. Gairaa K, Khellaf A, Messlem Y, Chellali F. Estimation of the daily global solar radiation based on Box–Jenkins and ANN models: A combined approach. *Renewable and Sustainable Energy Reviews* 2016; 57: 238-249, <http://dx.doi.org/10.1016/j.rser.2015.12.111>
32. Gharbia IB, Ferzly J, Vohralík M, Yousef S. Adaptive inexact smoothing Newton method for a nonconforming discretization of a variational inequality. *Computers & Mathematics with Applications*. 2023 Mar 1;133:12-29, <https://doi.org/10.1016/j.camwa.2022.11.031>
33. Geier N, Davim JP, Szalay T. Advanced cutting tools and technologies for drilling carbon fibre reinforced polymer (CFRP) composites: A

- review. *Composites Part A: Applied Science and Manufacturing* 2019; 125: 105552, <https://doi.org/10.1016/j.compositesa.2019.105552>
34. Guermoui M, Melgani F, Gairaa K, Mekhalfi ML. A comprehensive review of hybrid models for solar radiation forecasting. *Journal of Cleaner Production* 2020; 258: 120357, <http://dx.doi.org/10.1016/j.jclepro.2020.120357>
 35. Gouveia L, Paias A, Ponte M. The travelling salesman problem with positional consistency constraints: An Application to healthcare services. *European Journal of Operational Research*. 2023 Aug 1;308(3):960-89, <https://doi.org/10.1016/j.ejor.2022.11.050>
 36. Hajihassani, M., Jahed Armaghani, D., Monjezi, M., Mohamad, E.T. and Marto, A., 2015. Blast-induced air and ground vibration prediction: a particle swarm optimization-based artificial neural network approach. *Environmental Earth Sciences*, 74, pp.2799-2817. <https://doi.org/10.1007/s12665-015-4274-1>
 37. Hassan MA, Bailek N, Bouchouicha K, Nwokolo SC. Ultra-short-term exogenous forecasting of photovoltaic power production using genetically optimized non-linear auto-regressive recurrent neural networks. *Renewable Energy* 2021; 171: 191-209, <https://doi.org/10.1016/j.renene.2021.02.103>
 38. Hassani H, Yeganegi MR. Selecting optimal lag order in Ljung–Box test. *Physica A: Statistical Mechanics and its Applications* 2020; 541:123700, <https://doi.org/10.1016/j.physa.2019.123700>
 39. Hong D, Li G, Wei L, Li D, Li P, Yi Z. A self-scaling sequential quasi-Newton method for estimating the heat transfer coefficient distribution in the air jet impingement. *International Journal of Thermal Sciences*. 2023 Mar 1;185:108059, <https://doi.org/10.1016/j.ijthermalsci.2022.108059>
 40. Hong S, Hu X. Optimization of impeller of deep-sea mining pump for erosive wear reduction based on response surface methodology. *Marine Georesources & Geotechnology* 2022; 1-17, <https://doi.org/10.3390/jmse10081063>
 41. Hyder Z, Siau K, Nah F. Artificial intelligence, machine learning, and autonomous technologies in mining industry. *Journal of Database Management (JDM)* 2019; 30(2): pp.67-79, <https://doi.org/10.4018/JDM.2019040104>
 42. Ikemoto K, Takahashi K, Ozawa T, Isobe H. Akaike's Information Criterion for Stoichiometry Inference of Supramolecular Complexes. *Angewandte Chemie International Edition*. 2023 Mar 27;62(14):e202219059, <https://doi.org/10.1002/anie.202219059>
 43. Jiang X, Yang H, Yin J, Liao W. A three-term conjugate gradient algorithm with restart procedure to solve image restoration problems. *Journal of Computational and Applied Mathematics*. 2023 May 1;424:115020, <https://doi.org/10.1016/j.cam.2022.115020>
 44. Joe-Asare T, Stemm E, Amegbey N. Causal and contributing factors of accidents in the Ghanaian mining industry. *Safety Science*. 2023 Mar 1;159:106036, <https://doi.org/10.1016/j.ssci.2022.106036>
 45. Jung W, Taflanidis AA. Efficient global sensitivity analysis for high-dimensional outputs combining data-driven probability models and dimensionality reduction. *Reliability Engineering & System Safety*. 2023 Mar 1;231:108805, <https://doi.org/10.1016/j.res.2022.108805>
 46. Jurado-Molina J, Hernández-López CH, Hernández C. Evaluation of fish density influence on the growth of the spotted rose snapper reared in floating net cages using growth models and non-parametric tests. *Ciencias Marinas*. 2023 Jan 11, <https://doi.org/10.7773/cm.y2023.3253>
 47. Karsoliya S. Approximating number of hidden layer neurons in multiple hidden layer BPNN architecture. *International Journal of Engineering Trends and Technology* 2012; 3(6): 714-717, <http://www.ijettjournal.org/volume-3/issue-6/IJETT-V3I6P206.pdf>
 48. Kechaou F, Addouche SA, Zolghadri M. A comparative study of overall equipment effectiveness measurement systems. *Production Planning & Control* 2022; 1-20, <https://doi.org/10.1080/09537287.2022.2037166>
 49. Khanna P, Sahu M. Performance Analysis of Breast Cancer Data Using Mann–Whitney U Test and Machine Learning. In *Advances in Signal Processing, Embedded Systems and IoT: Proceedings of Seventh ICMEET-2022* 2023 May 24 (pp. 277-286). Singapore: Springer Nature Singapore, https://doi.org/10.1007/978-981-19-8865-3_26
 50. Khanduzi R, Sangaiah AK. An efficient recurrent neural network for defensive Stackelberg game. *Journal of Computational Science*. 2023 Mar 1;67:101970, <http://dx.doi.org/10.1016/j.jocs.2023.101970>
 51. Klyatis LM. Implementation Successful Prediction of Product Efficiency, Accelerated: Reliability and Durability Testing, and Accurate Simulation. In *Prediction Technologies for Improving Engineering Product Efficiency* 2023 Jan 4 (pp. 193-261). Cham: Springer International Publishing. https://doi.org/10.1007/978-3-031-16655-6_6
 52. Li Z, Wang J, Huang J, Ding M. Development and research of triangle-filter convolution neural network for fuel reloading optimization of block-type HTGRs. *Applied Soft Computing*. 2023 Mar 1;136:110126, <https://doi.org/10.1016/j.asoc.2023.110126>
 53. Liang H, Zou J, Zuo K, Khan MJ. An improved genetic algorithm optimization fuzzy controller applied to the wellhead back pressure

- control system. *Mechanical Systems and Signal Processing* 2020, 142: 106708, <http://dx.doi.org/10.1016/j.ymsp.2020.106708>
54. Lindegren ML, Lunau MR, Mafia MMP, da Silva ER. Combining simulation and data analytics for oee improvement. *International Journal of Simulation Modelling (IJSIMM)* 2022; 21(1), <https://doi.org/10.2507/IJSIMM21-1-584>
 55. Li H, Knapik S, Li Y, Park C, Guo J, Mojumder S, Lu Y, Chen W, Apley DW, Liu WK. Convolution Hierarchical Deep-Learning Neural Network Tensor Decomposition (C-HiDeNN-TD) for high-resolution topology optimization. *Computational Mechanics*. 2023 May 3:1-20, <https://doi.org/10.1007/s00466-023-02333-8>
 56. Liu, B., Yu, X., Chen, J. and Wang, Q., 2021. Air pollution concentration forecasting based on wavelet transform and combined weighting forecasting model. *Atmospheric Pollution Research*, 12(8), p.101144, <https://doi.org/10.1016/j.apr.2021.101144>
 57. Lourakis MI. A brief description of the Levenberg-Marquardt algorithm implemented by levmar. *Foundation of Research and Technology* 2005; 4(1): 1-6.
 58. Luo J, Wan L, Zhang Q, Cui B, Li C, Jiang Y, Jiang M, Wang K. Constructing a drug release model by central composite design to investigate the interaction between drugs and temperature-sensitive controlled release nanoparticles. *European Journal of Pharmaceutics and Biopharmaceutics*. 2023 Feb 1;183:24-32, <https://doi.org/10.1016/j.ejpb.2022.12.009>
 59. Luconi E, Boracchi P, Nodari R, Comandatore F, Marano G, Vaglianti F, Galli M, Biganzoli E. Spatial and Temporal Analyses of the Event of Death for 1480 in Milan Using the Data Contained in the Sforza's Registers of the Dead. *International Journal of Environmental Research and Public Health*. 2023 Feb 4;20(4):2783, <https://doi.org/10.3390/ijerph20042783>.
 60. Ma L, Meng Z, Teng Z, Tang Q. A measurement error prediction framework for smart meters under extreme natural environment stresses. *Electric Power Systems Research*. 2023 May 1;218:109192, <https://doi.org/10.1016/j.epsr.2023.109192>
 61. Makoni T, Mazuruse G, Nyagadza B. International tourist arrivals modelling and forecasting: A case of Zimbabwe. *Sustainable Technology and Entrepreneurship*. 2023 Jan 1;2(1):100027, <https://doi.org/10.1016/j.stae.2022.100027>
 62. Martins GS, Giesbrecht M. Clearness index forecasting: A comparative study between a stochastic realization method and a machine learning algorithm. *Renewable Energy* 2021; 180: 787-805, <https://doi.org/10.1016/j.renene.2021.08.094>
 63. Marey S, Aboukarima A, Almajhadi Y. Predicting the performance parameters of chisel plow using neural network model. *Engenharia Agrícola* 2020, 40: 719-731, <https://doi.org/10.1590/1809-4430-Eng.Agric.v40n6p719-731/2020>
 64. McKenzie E. Some ARMA models for dependent sequences of Poisson counts. *Advances in Applied Probability* 1988, 20(4): 822-835, <https://doi.org/10.2307/1427362>
 65. Mishra DP, Sugla M, Singha P. Productivity improvement in underground coal mines-a case study. *Journal of Sustainable Mining* 2013; 12(3): 48-53, <https://doi.org/10.46873/2300-3960.1300>
 66. Morrison WM, Tang R. China's rare earth industry and export regime: economic and trade implications for the United States 2012, <https://sgp.fas.org/crs/row/R42510.pdf>
 67. Montgomery DC. *Design and analysis of experiments*. John Wiley & sons 2017, ISBN: 978-1-119-49244-3
 68. Heckman JJ, Lochner LJ, Todd PE. Earnings functions, rates of return and treatment effects: The Mincer equation and beyond. *Handbook of the Economics of Education* 2006; 1: 307-458, [https://doi.org/10.1016/S1574-0692\(06\)01007-5](https://doi.org/10.1016/S1574-0692(06)01007-5)
 69. Hossain ME, Islam MR. *Drilling Engineering Problems and Solutions: A Field Guide for Engineers and Students*. John Wiley & Sons 2018, ISBN: 978-1-118-99864-9. <https://doi.org/10.1002/9781118998632>
 70. Nariyan E, Sillanpää M, Wolkersdorfer C. Uranium removal from Pyhäsalmi/Finland mine water by batch electrocoagulation and optimization with the response surface methodology. *Separation and Purification Technology* 2018; 193: pp.386-397, <https://doi.org/10.1016/j.seppur.2017.10.020>
 71. Palanikumar, K. Experimental investigation and optimisation in drilling of GFRP composites. *Measurement* 2011; 44(10): 2138-2148, <https://doi.org/10.1016/j.measurement.2011.07.023>
 72. Paventhan R, Lakshminarayanan PR, Balasubramanian V. Fatigue behaviour of friction welded medium carbon steel and austenitic stainless steel dissimilar joints. *Materials & Design* 2011, 32(4): 1888-1894, <https://doi.org/10.1016/j.matdes.2010.12.011>
 73. Patra AK, Gautam S, Majumdar S, Kumar P. Prediction of particulate matter concentration profile in an opencast copper mine in India using an artificial neural network model. *Air Quality, Atmosphere & Health* 2016; 9: 697-711. <https://doi.org/10.1007/s11869-015-0369-9>
 74. Pan Y, Chen L, Wang J, Ma H, Cai S, Pu S, Duan J, Gao L, Li E. Research on deformation prediction of tunnel surrounding rock using the

- model combining firefly algorithm and nonlinear auto-regressive dynamic neural network. *Engineering with Computers* 2021; 37: 1443-1453, <https://link.springer.com/article/10.1007/s00366-019-00894-y>.
75. Prasad BS, Murthy VMSR, Naik SR. Challenges in Drill Equipment Selection vis-à-vis Underground Excavations—A Methodology. In *Proceedings of Geotechnical Challenges in Mining, Tunneling and Underground Infrastructure 2022*, 167-182, 10.1007/978-981-16-9770-8_9.
 76. Raffaldi MJ, Seymour JB, Richardson J, Zahl E, Board M. Cemented paste backfill geomechanics at a narrow-vein underhand cut-and-fill mine. *Rock mechanics and rock engineering* 2019; 52: 4925-4940, <https://link.springer.com/article/10.1007/s00603-019-01850-4>.
 77. Raich A, Wu X, Cinar A. A comparative study of neural networks and nonlinear time series modeling techniques. In *Dynamics and Control of Chemical Reactors, Distillation Columns, and Batch Processes (DYCORD'92): Selected Papers from the 3rd IFAC Symposium, Maryland, USA, 26-29 April 1992*, 3: 63.
 78. Ratnayake RC. Challenges in inspection planning for maintenance of static mechanical equipment on ageing oil and gas production plants: The state of the art. In *International Conference on Offshore Mechanics and Arctic Engineering 2012*; 44939: 91-103, <http://dx.doi.org/10.1115/OMAE2012-83248>
 79. Robatto Simard S, Gamache M, Doyon-Poulin P. Current Practices for Preventive Maintenance and Expectations for Predictive Maintenance in East-Canadian Mines. *Mining*. 2023 Mar;3(1):26-53, <http://dx.doi.org/10.3390/mining3010002>
 80. Robèrt, K.H., Schmidt-Bleek, B., De Larderel, J.A., Basile, G., Jansen, J.L., Kuehr, R., Thomas, P.P., Suzuki, M., Hawken, P. and Wackernagel, M.. Strategic sustainable development—selection, design and synergies of applied tools. *Journal of Cleaner production* 2002, 10(3), pp.197-214, <https://doi.org/10.1016/j.jclepro.2016.04.059>
 81. Sakib N, Wuest T. Challenges and opportunities of condition-based predictive maintenance: a review. *Procedia Cirp* 2018; 78: 267-272, <https://doi.org/10.1016/j.procir.2018.08.318>
 82. Samatamba B, Zhang L, Besa B. Evaluating and optimizing the effectiveness of mining equipment; the case of Chibuluma South underground mine. *Journal of Cleaner Production* 2020; 252: 119697, <https://doi.org/10.1016/j.jclepro.2019.119697>
 83. Sameer HA, Gharghan SK, Mutlag AH. Hybridization of particle swarm optimization algorithm with neural network for COVID-19 using computerized tomography scan and clinical parameters. *The Journal of Engineering*. 2023 Jan;2023(2):e12226, <https://doi.org/10.1049/tje2.12226>
 84. Sarah Sarwar S. Comparison between the previous and current method of copex distribution and optimization of Robi Axiata Limited 2013, Brac University, Ayesha Abed Library.
 85. Sharma P, Said Z, Memon S, Elavarasan RM, Khalid M, Nguyen XP, Arc M, Hoang AT, Nguyen LH. Comparative evaluation of AI-based intelligent GEP and ANFIS models in prediction of thermophysical properties of Fe₃O₄-coated MWCNT hybrid nanofluids for potential application in energy systems. *International Journal of Energy Research* 2022; 46(13): 19242-19257, <https://doi.org/10.1002/er.8010>
 86. Shamshirband S, Mohammadi K, Yee L, Petković D, Mostafaepour A. A comparative evaluation for identifying the suitability of extreme learning machine to predict horizontal global solar radiation. *Renewable and sustainable energy reviews* 2015; 52: 1031-1042, <http://dx.doi.org/10.1016/j.rser.2015.07.173>
 87. Sheykhi H, Bagherpour R, Ghasemi E, Kalhori H. Forecasting ground vibration due to rock blasting: a hybrid intelligent approach using support vector regression and fuzzy C-means clustering. *Engineering with Computers* 2018; 34: 357-365, <https://doi.org/10.1007/s00366-017-0546-6>
 88. Sick B. Online tool wear monitoring in turning using time-delay neural networks. In *Proceedings of the 1998 IEEE International Conference on Acoustics, Speech and Signal Processing, ICASSP'98 (Cat. No. 98CH36181)*, 1: 445-448, <https://doi.org/10.1007/BF01428126>
 89. Soltani ER, Panahi HA, Moniri E, Fard NT, Raeisi I, Beik J, Siavoshani AY. Construction of a pH/Temperature dual-responsive drug delivery platform based on exfoliated MoS₂ nanosheets for effective delivery of doxorubicin: Parametric optimization via central composite design. *Materials Chemistry and Physics*. 2023 Feb 1;295:127159, <https://doi.org/10.1016/j.matchemphys.2022.127159>
 90. Sun P, Zhou S, Cao H, Cai G, Zhang S, Gao Q, Cheng G, Liu B, Liu G, Zhang X, Liu Y. Design and Implementation of a Chain-Type Direct Push Drilling Rig for Contaminated Sites. *International Journal of Environmental Research and Public Health*. 2023 Feb 20;20(4):3757, <https://doi.org/10.3390/ijerph20043757>

91. Sun Y, Liu Y, Qin X, Dou Z, Feng Z, Yang G. Investigating Drillstring Vibration and Stability in Coring Drilling. *Energies* 2022; 15(14): 5234, <https://doi.org/10.3390/en15145234>
92. Talalay PG. Perspectives for development of ice-core drilling technology: a discussion. *Annals of Glaciology*. 2014;55(68):339-50, <https://doi.org/10.3189/2014AoG68A007>
93. Talalay PG. Rigs and Drills for Geotechnical and Exploration Rotary Drilling in the Polar Regions. In *Geotechnical and Exploration Drilling in the Polar Regions 2023 Jan 2* (pp. 259-294). Cham: Springer International Publishing. https://doi.org/10.1007/978-3-031-07269-7_9
94. Tao W, Jiang F, Li L, Zhang D, Guo X, Liao WH. Dynamical analysis and vibration estimation of a flexible plate with enhanced active constrained layer damping treatment by combinatorial neural networks of surrogates. *Aerospace Science and Technology*. 2023 Jan 17:108136, <https://doi.org/10.1016/j.ast.2023.108136>.
95. Tian J, Li J, Cheng W, Zhu Z, Yang L, Yang Y, Zhang T. Working mechanism and rock-breaking characteristics of coring drill bit. *Journal of Petroleum Science and Engineering*. 2018 Mar 1;162:348-57, <https://doi.org/10.1016/j.petrol.2017.12.047>.
96. Tiwari, P., 2023. Effect of innovation practices of banks on customer loyalty: an SEM-ANN approach. *Benchmarking: An International Journal*, (ahead-of-print), <https://doi.org/10.1108/BIJ-06-2022-0392>
97. Toper AZ, Kabongo KK, Stewart RD, Daehnke A. The mechanism, optimization and effects of preconditioning. *Journal of the Southern African Institute of Mining and Metallurgy* 2000, 100(1): 7-15.
98. Verano DA, Husnawati H, Ermatita E. Implementation of autoregressive integrated moving average model to forecast raw material stock in the digital printing industry. *Journal of Information Technology and Computer Science* 2020, 5(1): 13-22, <http://dx.doi.org/10.25126/jitecs.202051117>
99. Wang H, Tenorio V, Li G, Hou J, Hu N. Optimization of trackless equipment scheduling in underground mines using genetic algorithms. *Mining, Metallurgy & Exploration*. 2020; 37:1531-44, <http://dx.doi.org/10.1007/s42461-020-00285-8>
100. Weremfo A, Abassah-Oppong S, Adulley F, Dabie K, Seidu-Larry S. Response surface methodology as a tool to optimize the extraction of bioactive compounds from plant sources. *Journal of the Science of Food and Agriculture*. 2023 Jan 15;103(1):26-36, <https://doi.org/10.1002/jsfa.12121>
101. Woodroffe NJ, Ariaratnam ST. Cost and risk evaluation for horizontal directional drilling versus open cut in an urban environment. *Practice periodical on structural design and construction* 2008; 13(2): 85-92. [https://doi.org/10.1061/\(ASCE\)1084-0680\(2008\)13:2\(85\)](https://doi.org/10.1061/(ASCE)1084-0680(2008)13:2(85))
102. Woodward DG. Life cycle costing—Theory, information acquisition and application. *International journal of project management* 1997; 15(6): 335-344, [https://doi.org/10.1016/S0263-7863\(96\)00089-0](https://doi.org/10.1016/S0263-7863(96)00089-0)
103. Wu CL, Chau KW. Prediction of rainfall time series using modular soft computing methods. *Engineering applications of artificial intelligence* 2013; 26(3): 997-1007, <https://doi.org/10.1016/j.engappai.2012.05.023>
104. Wu Y, Liu L, Qian S. A small sample bearing fault diagnosis method based on variational mode decomposition, autocorrelation function, and convolutional neural network. *The International Journal of Advanced Manufacturing Technology*. 2023 Feb;124(11-12):3887-98, <https://doi.org/10.1007/s00170-021-08126-8>
105. Xie Y, Wang S, Zhang G, Fan Y, Fernandez C, Blaabjerg F. Optimized multi-hidden layer long short-term memory modeling and suboptimal fading extended Kalman filtering strategies for the synthetic state of charge estimation of lithium-ion batteries. *Applied Energy*. 2023 Apr 15;336:120866, <https://doi.org/10.1016/j.apenergy.2023.120866>
106. Ye Y, Huang Q, Rong Y, Yu X, Liang W, Chen Y, Xiong S. Field detection of small pests through stochastic gradient descent with genetic algorithm. *Computers and Electronics in Agriculture*. 2023 Mar 1;206:107694, <https://doi.org/10.1016/j.compag.2023.107694>
107. Yin M, He S, Soomro TA, Yuan H. Efficient skeleton-based action recognition via multi-stream depthwise separable convolutional neural network. *Expert Systems with Applications*. 2023 Sep 15;226:120080, <http://dx.doi.org/10.1016/j.eswa.2023.120080>
108. Zaki MJ. SPADE: An efficient algorithm for mining frequent sequences. *Machine learning* 2001; 42: 31-60, <https://doi.org/10.1023/A:1007652502315>
109. Zhang JL, Liu X, Ren TY, Yuan Y, Mang HA. Structural behavior of reinforced concrete segments of tunnel linings strengthened by a steel-concrete composite. *Composites Part B: Engineering* 2019; 178: 107444, <http://dx.doi.org/10.1016/j.compositesb.2019.107444>
110. Zhao R, Shi S, Li S, Guo W, Zhang T, Li X, Lu J. Deep Learning for Intelligent Prediction of Rock Strength by Adopting Measurement While Drilling Data. *International Journal of Geomechanics*. 2023 Apr 1;23(4):04023028, <https://doi.org/10.1061/IJGNAI.GMENG-8080>

111. Zuo HY, Luo ZQ, Guan JL, Wang YW. Identification on rock and soil parameters for vibration drilling rock in metal mine based on fuzzy least square support vector machine. *Journal of Central South University* 2014; 21(3): 1085-1090, <http://dx.doi.org/10.1007/s11771-014-2040-2>